Int J Earth Sci (Geol Rundsch) (2011) 100:753–785
DOI 10.1007/s00531-010-0512-7

ORIGINAL PAPER

Hot metamorphic core complex in a cold foreland

Wolfgang Franke · Michael Patrick Doublier · Kai Klama · Sébastien Potel · Klaus Wemmer

Received: 13 February 2007 / Accepted: 19 December 2009 / Published online: 20 April 2010

Abstract The Montagne Noire forms the southernmost part of the French Massif Central. Carboniferous flysch sediments and very low-grade metamorphic imprint testify to a very external position in the orogen. Sedimentation of synorogenic clastic sediments continued up to the Viséan/Namurian boundary (≤320 Ma). Subsequently, the Palaeozoic sedimentary pile underwent recumbent folding and grossly southward thrusting. An extensional window exposes a hot core of Carboniferous HT/LP gneisses, migmatites and granites (Zone Axiale), which was uplifted from under the nappe pile. After the emplacement of the nappes on the Zone Axiale (Variscan D_1), all structural levels shared the same tectonic evolution: D_2 (extension and exhumation), D_3 (refolding) and post-D_3 dextral transtension. HT/LP-metamorphism in the crystalline rocks probably started before and continued after the emplacement of the nappes. Peak metamorphic temperatures were attained during a post-nappe thermal increment (M_2). M_2 occurred during ENE-directed bilateral extension, which exhumed the Zone Axiale and its frame as a ductile horst structure, flanked to the ENE by a Stephanian intra-montane basin. Map patterns and mesoscopic structures reveal that extension in ENE occurred simultaneously with NNW-oriented shortening. Combination of these D_2 effects defines a bulk prolate strain in a "pinched pull-apart" setting. Ductile D_2 deformation during M_2 dominates the structural record. In wide parts of the nappes on the southern flank of the Zone Axiale, D_1 is only represented by the inverted position of bedding (overturned limbs of recumbent D_1 folds) and by refolded D_1 folds. U–Pb monazite and zircon ages and K–Ar muscovite ages are in accord with Ar–Ar data from the literature. HT/LP metamorphism and granitoid intrusion commenced already at ≥330 Ma and continued until 297 Ma, and probably in a separate pulse in post-Stephanian time. Metamorphic ages older than c. 300 Ma are not compatible with the classical model of thermal relaxation after stacking, since they either pre-date or too closely post-date the end of flysch sedimentation. We therefore propose that migmatization and granite melt generation were independent from crustal thickening and caused, instead, by the repeated intrusion of melts into a crustal-scale strike-slip shear zone. Advective heating continued in a pull-apart setting whose activity outlasted the emplacement of the Variscan nappe pile. The shear-zone model is confirmed by similar orogen-parallel extensional windows with HT/LP metamorphism and granitoid intrusion in neighbouring areas, whose location is independent from their position in the orogen. We propose that heat transfer from the mantle occurred in dextral strike-slip shear zones controlled by the westward

W. Franke (✉) · K. Klama
Institut für Geowissenschaften der Johann Wolfgang Goethe-Universität, Altenhöferallee 1, 60438 Frankfurt, Germany
e-mail: w.franke@em.uni-frankfurt.de

M. P. Doublier
Geological Survey of Western Australia, Cnr Hunter and Broadwood Street, 6430 Kalgoorlie, WA, Australia

S. Potel
Institut Polytechnique La Salle Beauvais, 19 rue Pierre Waguet, BP 30313, 60026 Beauvais Cedex, France

K. Wemmer
Geowissenschaftliches Zentrum der Georg-August Universität, Goldschmidtstraße 1-3, 37077 Göttingen, Germany

propagating rift of the Palaeotethys ocean, which helped to destroy the Variscan orogen.

Keywords Metamorphic core complex · Orogen-parallel extension · HT/LP metamorphism · Granitoids · Carboniferous · Montagne Noire · France · Variscides

Introduction

The Montagne Noire at the southern margin of the French Massif Central represents an external part of the Variscan orogen, characterized by foreland flysch sediments and weakly metamorphosed, highly fossiliferous Palaeozoic sediments. Ever since a benchmark paper by Gèze et al. (1952), the area has been regarded as a classical case of Variscan nappe tectonics. Engel et al. (1978, 1981) have studied, in this area, systematic relationships between tectonic stacking and flysch sedimentation. During the last decade, attention has focused upon the crystalline Zone Axiale, which rises from under the weakly metamorphosed sediments of the foreland. Isotopic ages reveal that the Zone Axiale underwent metamorphism in Carboniferous time. This precludes comparison with uplifts of old and cold basement such as, e.g., the external massifs in the foreland of the Western Alps. For the origin of this "hot" gneissic core, a multitude of models have been proposed, most of which invoke extension during gravitational collapse of previously thickened crust. In this paper, we present new tectonic observations and isotopic ages mainly from the eastern Montagne Noire. This data set and comparisons with neighbouring areas permit to derive a new geodynamic model for the late- and post-orogenic processes active in large parts of the mid-European Variscides.

We dedicate this paper to the memory of Wolfgang Engel, who has made important contributions toward the sedimentology of turbidites as well as to the Carboniferous palaeogeography, very low-grade metamorphism and tectonic evolution of the Rhenish Massif, Montagne Noire and Pyrenees.

Geological setting

The Montagne Noire is situated at the southern margin of the French Massif Central, on the southern flank of the Variscan Belt. The tectonic architecture of the Massif Central reveals widespread metamorphic inversion by southward-directed post-metamorphic thrusting. Metamorphic grade decreases down-section and toward the South (e.g., Matte 1991; Faure et al. 2009). In accordance

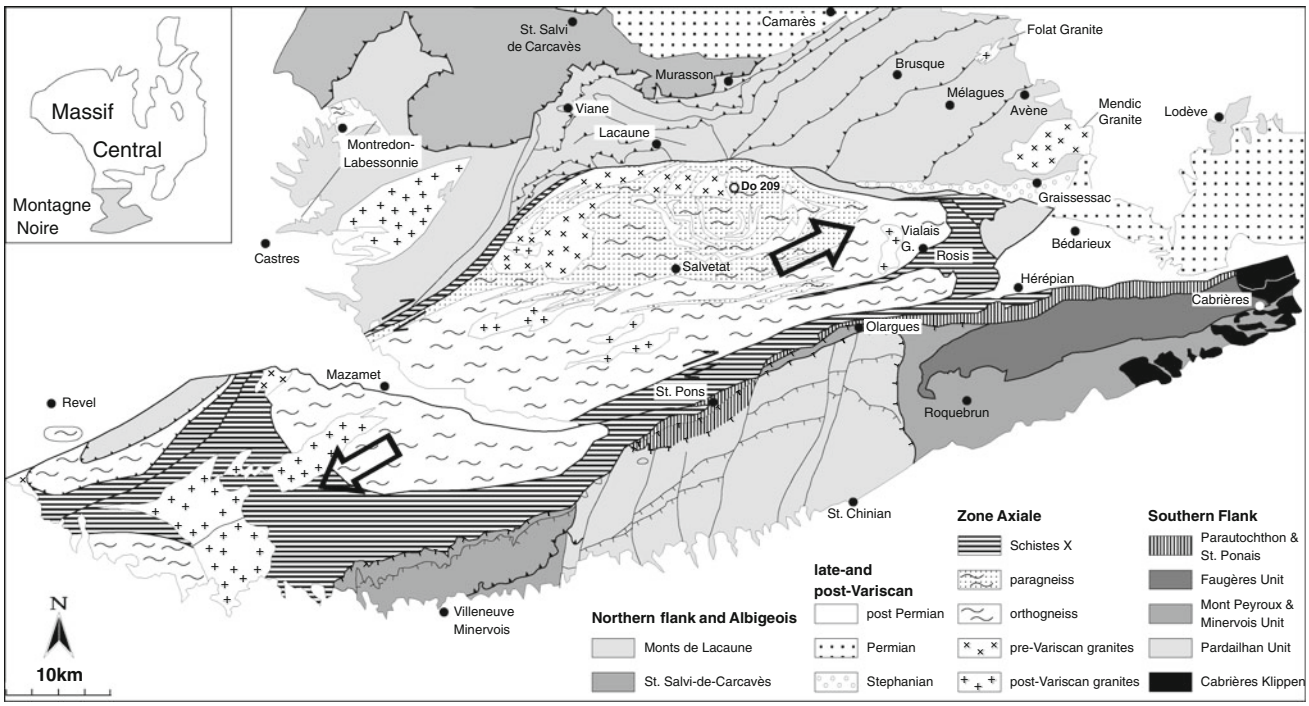

Fig. 1 Geological sketch map of the Montagne Noire (after Doublier et al. 2006, based upon Guérangé-Lozes and Burg 1990; Demange et al. 1995; Alabouvette et al. 2003). *Open arrows* bipolar ductile shear after Mattauer et al. (1996). Do 209: geochronology sample (see text). *Inset* position of the Montagne Noire at the southern extremity of the Massif Central

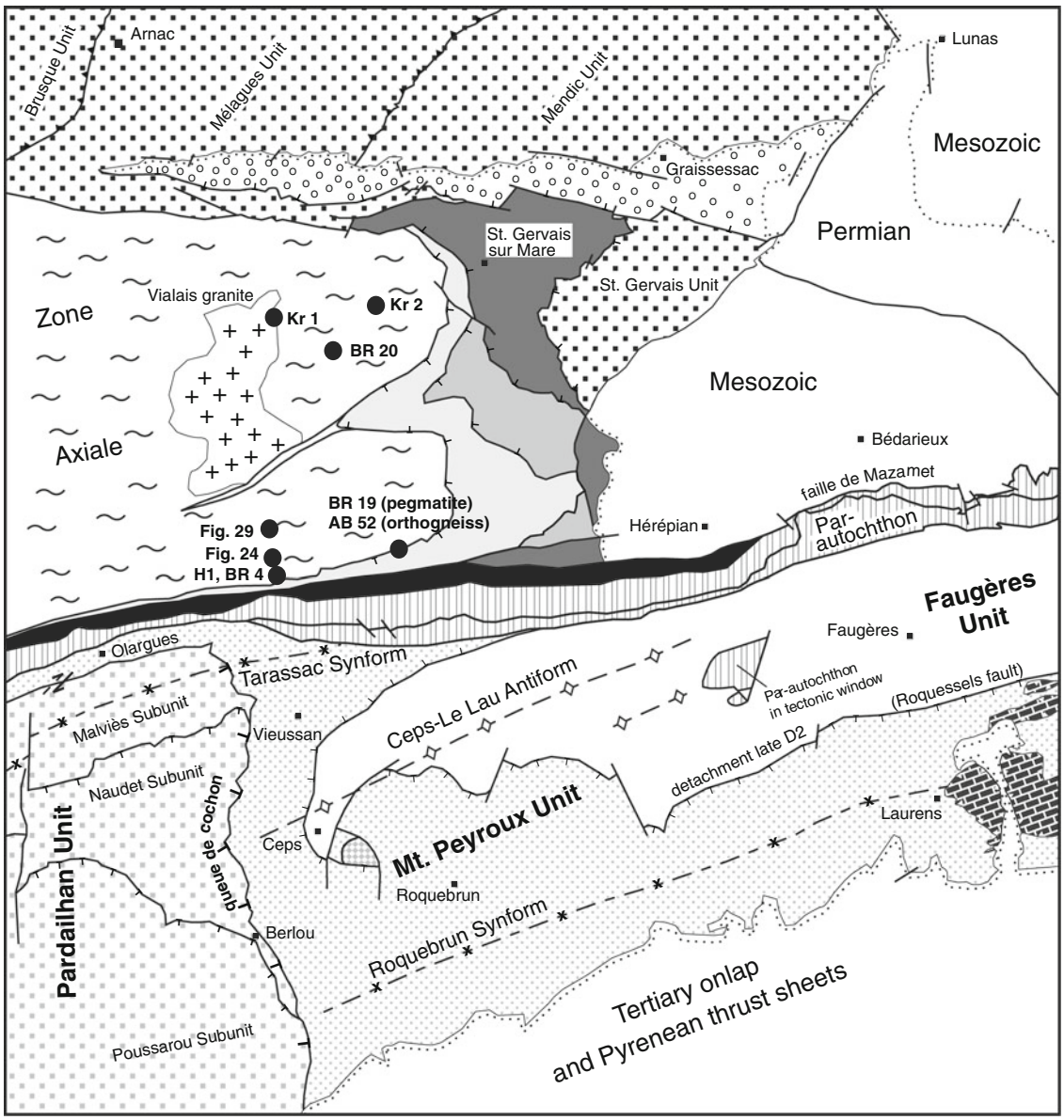

Fig. 2 Structural map of the eastern Montagne Noire, with the position of outcrops Figs. 24, 29 and further geochronological sampling sites (see text)

with its external position in the orogen, the Montagne Noire contains sedimentary rocks of low to very low metamorphic grade, including widespread synorogenic clastic sediments of Carboniferous age (Engel et al. 1978, 1981).

This regular pattern is disrupted by a metamorphic dome structure—the Zone Axiale—which emerges from under the lower-grade cover (Figs. 1, 2). In the eastern part of the Zone Axiale, the metamorphic foliation defines a double antiform (e.g., Béaud 1985; Demange 1998; Matte et al. 1998) with the Espinouse dome to the north and the Caroux dome to the south, separated by the Rosis synform (Figs. 2, 3). Westwards, the synform is affected by a shear zone (Schranzhofer 1999). The Espinouse dome is wider and exposes deeper metamorphic levels with widespread anatexis and granitoids. The lowermost structural levels of the Zone Axiale are occupied by calc-alkaline ortho-augengneisses (mainly migmatic), with subordinate intercalations of metasediments, mafic rocks and—locally—boudins of retrogressed ultramafic rocks and eclogites.

U–Pb dating of the orthogneisses has yielded a variety of Ordovician protolith ages: c. 440 Ma (U–Pb SHRIMP, Gebauer et al. 1988), 450 ± 6 and 456 ± 3 Ma (U–Pb TIMS, Roger et al. 2004), 456 ± 2 Ma (U–Pb TIMS, concordant zircon, Blatt et al. 2005), 458 ± 9 Ma (microprobe on monazite xenocryst in Carboniferous migmatite,

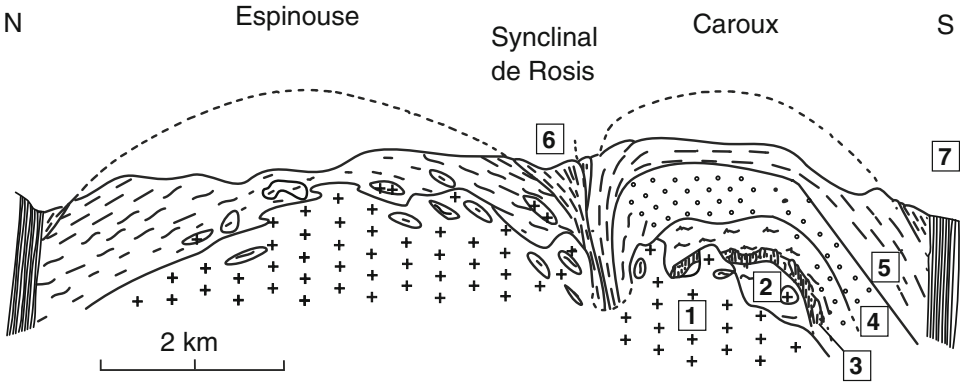

Fig. 3 Tectonic section across the Zone Axiale of the eastern Montagne Noire (after Béaud 1985). *1* anatectic granite, *2* ortho-augengneiss, *3* migmatic paragneiss with mafic boudins, *4* migmatites and diatexites with sillimanite nodules, *5* ortho-augengneiss, *6* Schistes X, *7* late dextral shear zone

Be Mezeme 2005), and 471 ± 4 Ma (U–Pb SHRIMP, Cocherie et al. 2005). The geodynamic setting of the Ordovician orthogneisses is being debated (Mattauer 2004).

The orthogneisses of the Zone Axiale are mantled by metasediments and subordinate metavolcanic rocks. Since their protolith ages are largely unknown, they have been termed "Schistes X". Blatt et al. (2005) dated a granitic orthogneiss sheet within paragneisses of the Schistes X3 (gneiss du Vernet) in the southern part of the Gorges de Colombières (sample AB 52 in Fig. 2): a discordant array of zircons yielded a U–Pb upper intercept age of 538 ± 34 Ma, which corresponds to the latest Proterozoic or Cambrian. A similar age of 545 ± 15 Ma has been reported from greenschist grade meta-dacites in the "Schistes X" at the southern margin of the Zone Axiale (Lescuyer and Cocherie 1992). Both these datings match part of the latest Proterozoic/Cambrian xenocryst ages from the gneissic core (Be Mezeme 2005). The meta-magmatic rocks either overly or else intrude an older (?Cadomian) basement, whose structure and metamorphic grade are unknown because of the strong Variscan overprint.

The *metamorphic evolution of the Zone Axiale* is polyphase. An earlier stage of medium-pressure metamorphism is represented in relict kyanite and even eclogites, the latter developed from ultramafic cumulates at 0.9 GPa (Demange 1985). We have re-calculated the P–T conditions for the eclogites, with the whole rock and mineral compositions published by Demange, the thermodynamic program THERIAK-DOMINO (based on the minimization of the Gibbs free energy) and the dataset of Holland and Powell (1998, updated 14 May 2001). For the omphacite–garnet–quartz–rutile assemblages at Carbard and Le Jounié, we obtained a minimum peak pressure of c. 1.4 GPa and a minimum peak temperature of c. 650°C. U–Pb zircon dating of eclogites yielded c. 440 Ma (Gebauer et al. 1988). However, this late Ordovician age for high-pressure metamorphism is not compatible with the Palaeozoic sedimentary record (see below).

The high and medium grade metamorphic relicts were strongly overprinted by Variscan LP/HT metamorphism up to anatectic grade (e.g., Bard and Rambeloson 1973; Thompson and Bard 1983; Ourzik et al. 1991). This evolution culminated in widespread migmatization and the intrusion of late- to post-tectonic granitoids. These high-temperature processes have been dated at ≥ 330 to c. 280 Ma (Rb–Sr whole rock, Hamet and Allègre 1976; U–Pb, Be Mezeme 2005; Matte et al. 1998). Gebauer et al. (1988) dated migmatic orthogneisses N of St. Pons at 308 Ma (U–Pb TIMS on monazite). In the eastern Espinouse dome, Krause et al. (2004), dated a "Roc Noir Granite" at c. 308 Ma and contact metamorphic events in orthogneiss (U–Pb TIMS on monazite, 316–313 Ma and c. 308 Ma) (samples Kr 1 and Kr 2 in Fig. 2, location after Doublier et al. 2006). The Folat Granite NE of the Zone Axiale has been dated at 314 ± 8 Ma (U–Pb TIMS on zircon fractions, Lévêque 1986). It seals the fault contact between the Brusque and Mélagues Palaeozoic units on the northern flank of the Zone Axiale (Fig. 1). The allegedly post-tectonic Vialais Granite in the eastern part of the Zone Axiale (Fig. 1) has yielded a U–Pb monazite age of 327 ± 4 Ma (Matte et al. 1998).

Maluski et al. (1991) have published Ar–Ar ages from the eastern part of the Zone Axiale. Migmatic orthogneiss from the Espinouse Dome yielded biotite at 316 Ma and a young generation of muscovite (300 Ma). In the shear belt (mainly Schistes X) at the southern margin of the Zone Axiale, biotite and muscovite range between 311 and 308 Ma, with one older sample at 314 Ma (hornblende) and 311 Ma (biotite), and one clearly younger sample with muscovite and biotite both at 303 Ma. The detachments fault zone at the base of the Palaeozoic sediments on both flanks of the Zone Axiale yielded 297 Ma.

The metamorphic grade of the Schistes X decreases up-section and towards the flanks of the dome structure. At a large scale, transition into the fossiliferous Palaeozoic sequences in the mantle of the Zone Axiale appears gradational (see metamorphic map in Demange 1985). However, existing maps reveal metamorphic breaks brought

about by ductile and brittle extensional faults. The vertical distance between migmatic gneisses and fossiliferous sediments is locally reduced to only c. 1.5 km (Figs. 2, 3).

The *Palaeozoic rocks* of the Montagne Noire are best preserved on the southern flank of the Zone Axiale (Fig. 2). The sequence is palaeontologically well dated and laterally consistent over large areas. This has permitted to identify large-scale recumbent folds and tectonic repetition by thrusting. Tectonic transport during this phase (D_1) was grossly directed towards the South. For a long time, these nappe structures have been regarded as the main tectonic event of the Montagne Noire (e.g., Arthaud 1970; Engel et al. 1981). However, later studies have revealed that the subsequent extensional phase (D_2) was equally or even more important (e.g., Echtler 1990). Although the original nappe pile has been strongly reduced by extension, it is still possible to reconstruct the entire palaeogeographic evolution from the Early Cambrian through to the Namurian sedimentary rocks.

The sequence starts with a thick pile of Early Cambrian shelf sandstones and carbonates, overlain by Middle Cambrian through Early Ordovician clastic sediments, all of which were deposited at the N-Gondwana margin (e.g., Feist et al. 1994; Piqué et al. 1994).

In most parts of the southern flank, Late Ordovician and Silurian deposits are missing. The Devonian oversteps the early Palaeozoic sequences with an angular unconformity of 10–30°. Gebauer and Grünenfelder (1976) have reported U–Pb ages on zircon fractions and Rb–Sr whole rock ages from metamorphic rocks of the Zone Axiale ranging between 445 ± 10 and 417 ± c. 35 Ma. These features might be taken to indicate a "Caledonian" orogenic event. However, the early Palaeozoic rocks on the southern flank of the Zone Axiale do not show a pre-Devonian folding or cleavage, and the Cabrières Klippen of the southeastern-most Montagne Noire (see below) contain a stratigraphic sequence without any angular unconformity (Feist and Schönlaub 1974). These features clearly argue against a "Caledonian" orogeny in the Montagne Noire, and rather suggest localized extensional uplift and subsequent marine transgression.

The sequence of the Cabrières Klippen includes rhyolites and andesites intercalated between marine clastic sediments of early Arenig and Caradoc age (Gonord et al. 1964). This corresponds to a span of absolute ages (c. 480–455 Ma, see Gradstein et al. 2004), which overlaps with the mid-/late Ordovician isotopic ages of the orthogneisses in the Zone Axiale.

Apart from a basal siliciclastic member, the Devonian sequence is entirely composed of carbonates. Depositional environments show a clear trend of upward deepening, from sabkha-type early diagenetic dolomites (Gedinnian to Pragian) over biodetrital limestones (Pragian to Eifelian) to hemipelagic nodular limestones (Late Eifelian through to the basal Carboniferous, Feist 1985). These limestones are overlain by black radiolarian cherts (Tournaisian), limestone turbidites and grey-green shales (early to mid-Viséan), and a debris flow member with limestone clasts ("schistes troués", late Viséan). The sedimentary record is terminated by a thick sequence of synorogenic, deep-water clastic sediments (flysch) of latest Viséan to Namurian A age (Engel et al. 1978, 1981; Feist and Galtier 1985; Aretz 2002).

It is important to know that the Palaeozoic sequence of the Montagne Noire is representative of a large and apparently coherent palaeogeographic domain. Similar Devonian and early Carboniferous sediments are also known from the basement of the Aquitaine basin (Paris and Le Pochat 1994), from the Mouthoumet Massif further South and from the Pyrenees. It can be stated that all of present-day southwestern and southern France was an area of marine sedimentation during the Devonian and Early Carboniferous, and represented the foreland to the southward driving orogenic wedge of the Massif Central.

The *north flank of the Zone Axiale* consists of Cambrian through to Silurian sedimentary rocks. Along the northwestern margin of the Zone Axiale, these rocks reveal HT/LP metamorphism decreasing away from the crystalline core. NE of the Zone Axiale (Eastern Monts de Lacaune), Cambrian and Ordovician sediments are repeated by SE-facing folds and thrusts. This association is of very low grade and is juxtaposed against the high-grade rocks of the gneissic core (Doublier et al. 2006). On both the north and the south flank of the Zone Axiale, the lower grade sedimentary rocks abut against the gneissic core along ENE-trending, dextral transtensional faults (e.g., Echtler 1990).

The northeastern termination of the Zone Axiale is a brittle/ductile, extensional fault system (e.g., Maluski et al. 1991), which forms the southwestern boundary of a half-graben filled with coal-bearing clastic sequences (Stephanian Graissessac basin). U–Pb ion microprobe dating of zircon from an intercalated ash layer has yielded an age of 295.5 ± 5.1 Ma (Bruguier et al. 2003).

The importance of extensional features has qualified the Montagne Noire, for several authors, as a prime example of "orogenic collapse", due to gravitational instability after tectonic thickening (e.g., van den Driessche and Brun 1992; Aerden 1998; Aerden and Malavieille 1999), possibly aided by strike-slip faulting (Echtler 1990; Echtler and Malavieille 1990). Alternatively, the Zone Axiale has been interpreted as a conical fold (Mattauer et al. 1996), a transpressive feature (Demange 1999), as a diapiric uplift (e.g., Faure and Cottereau 1988; Faure 1995), or else by a combination of diapirism and extensional collapse (Soula et al. 2001).

Structural geology

General features

Previous papers (e.g., Arthaud 1970; Echtler 1990; Echtler and Malavieille 1990; Matte et al. 1998; Aerden and Malavieille 1999; Demange 1998; Engel et al. 1981) have described several tectonic events, which we re-group, in this paper, into four main stages of the tectonic evolution (Fig. 4).

D_1: Recumbent folding and grossly S-directed nappe stacking

D_2: Extension in ENE (dominant synmetamorphic foliation and lineation, subsequent shortening in NNW)

D_3: Refolding into ENE-trending, upright folds. Like D_1, D_3 is due to the long-lasting, grossly N-directed shortening in the southern periphery of the orogen. We define D_3 as the late increment of the resulting deformation, which outlasted extensional D_2

post-D_3: Late extensional "collapse" folds, late dextral transtensional faults, NW-trending kinkfolds

As discussed below, these deformational increments are not discrete, regionally pervasive and isochronous events, but overlap in time and space (Fig. 4). Higher tectonic units have undergone D_1 deformation earlier than lower ones. Extensional deformation D_2 in the eastern part of the Montagne Noire migrated eastwards and up-section. In the highest unit (Mt. Peyroux), S_2 affected rocks already tilted by earlier increments of NNW-directed compression.

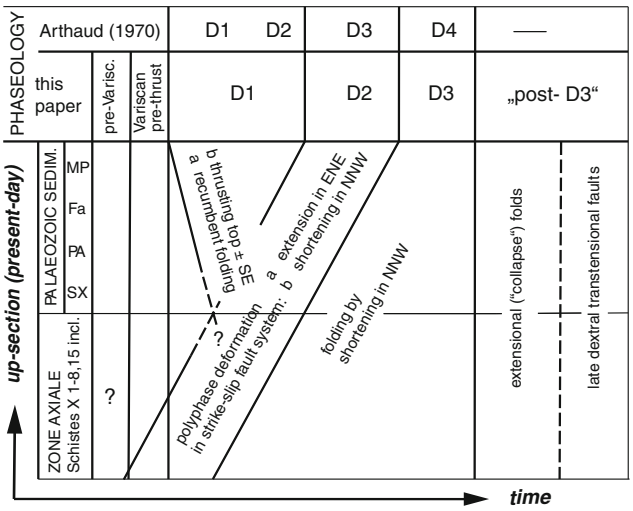

Fig. 4 Sequence of deformation phases in the SE part of the Montagne Noire, at different structural levels. *SX* higher Schistes X with presumably Palaeozoic protoliths, *PA* Par-Autochthon, *Fa* Faugères Unit, *MP* Mont Peyroux Unit

Structural relations between tectonic units

Reconstruction of the accretionary wedge (D_1)

Detailed mapping of large parts of the southeastern Montagne Noire and the findings of Doublier et al. (2006) from the northern flank permit a reappraisal of the large-scale structural relationships acquired during D_1. The Palaeozoic sediments on the southern flank of the Montagne Noire, have been subdivided into several tectonic units, which evolved from recumbent fold nappes (Arthaud 1970), but are separated, today, by extensional or transtensional faults (see below). We have not been able to identify primary nappe thrusts. We therefore prefer the term "tectonic unit" to the conventional designation as "nappes". These tectonic units are, in order from N to S and from bottom to top (Figs. 5, 6):

- *Parautochthon*: biotite-grade metapelites with subordinate meta-sandstones (?Ordovician), overlain to the south by meta-carbonates (Devonian), meta-cherts and meta-pelites (both Carboniferous). The structural thickness of the unit is less than 1 km. Carboniferous schists and pebbly mudstones belonging to the Parautochthon also occur in tectonic windows under the Faugères Unit W of Faugères (see Fig. 2 and geol. map 1:50,000 St. Chinian, Alabouvette et al. 1981).
- *Faugères Unit*: Devonian and Carboniferous sedimentary rocks of very low metamorphic grade, in both normal and inverted limbs of former D_1 folds. The structural thickness of the Faugères Unit unit W of Faugères amounts to 1–1.5 km.
- *Mont Peyroux Unit* (including the olistoliths of the Cabrières Klippen, see Engel et al. 1978, 1981): Ordovician, Devonian and Carboniferous sedimentary rocks of anchizonal to diagenetic grade. The Mont Peyroux Unit exhibits a large, ESE-facing D_1 fold, refolded by a later event (Engel et al. 1978, 1981). W of the Orb valley, the structural thickness of the Mt. Peyroux Unit is reduced by the late "queue de cochon" normal fault (see below). Further E, the cumulative thickness amounts to ≥4 km.
  The Devonian and Carboniferous rocks in the Faugères and Mt. Peyroux Units largely exhibit the same lithostratigraphic sequence. The main difference lies in the sedimentological character of the latest Viséan flysch, which shows much coarser-grained gravity flow deposits in the Mt. Peyroux (Engel et al. 1978, 1981). The *Minervois Unit*, a tectono-stratigraphic equivalent of the Mont Peyroux Unit in the western Montagne Noire, is not part of this study.
- *Pardailhan Unit*: Cambrian, Ordovician, and (locally) Devonian sedimentary rocks of anchizonal to

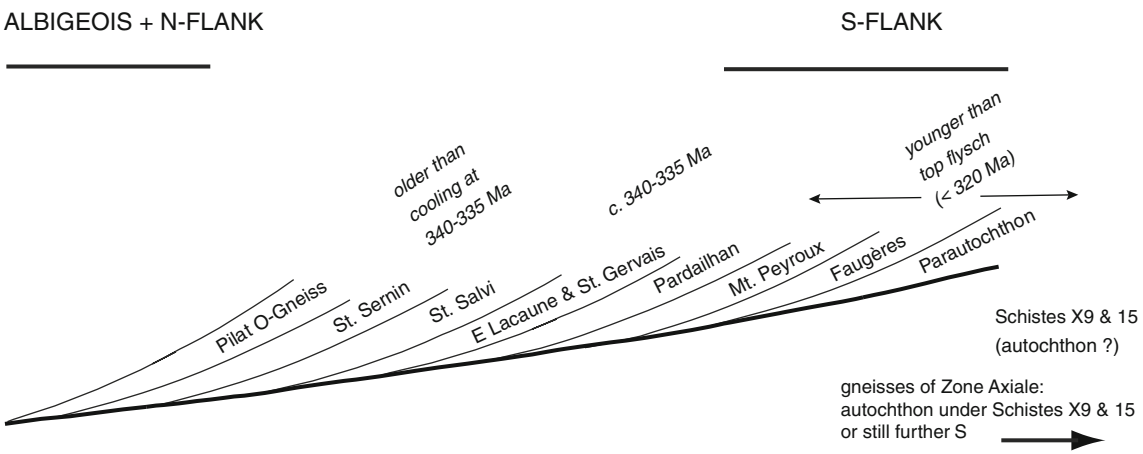

Fig. 5 Diagrammatic reconstruction of the accretionary tectonic wedge formed at the southern margin of the Massif Central during Variscan D_1 deformation, with its position relative to the present-day Zone Axiale and ages of D_1 deformation (*in italics*)

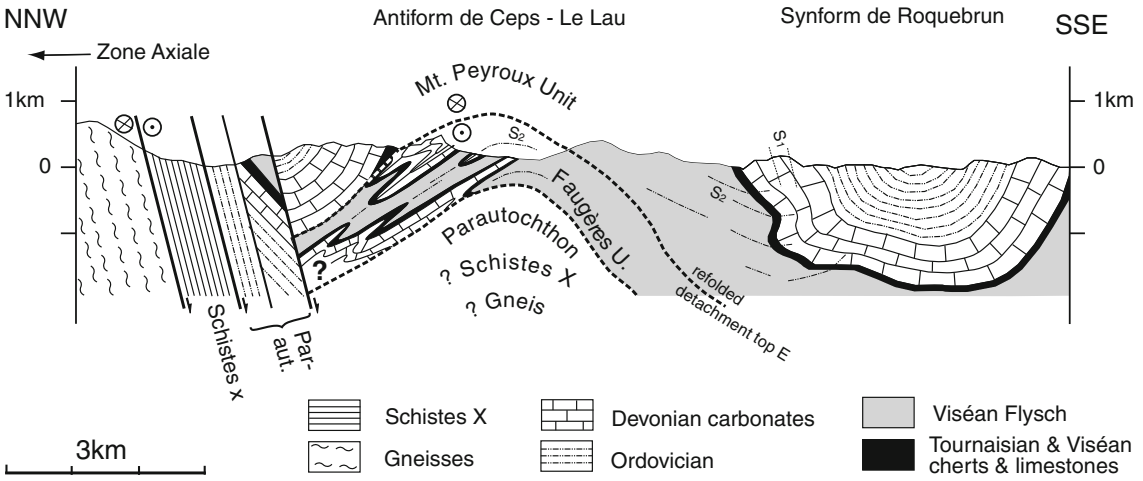

Fig. 6 Tectonic section across the southern flank of the Montagne Noire (modified after Wiederer et al. 2002). *Broken lines* trace of S_{2a} cleavage

diagenetic grade (Alabouvette et al. 1982). They represent the overturned limb and hinge of a large D_1 fold nappe facing downward to the South (Echtler 1990). The structural thickness of the unit W of the "queue de cochon" amounts to at least 3 km.

The accretionary sequence of these units and their spatial relation with areas to the North is depicted in Fig. 5. Unstacking follows the basic principle, which transforms the vertical tectonic sequence into a lateral sequence in the same order. This brings the highest units—Eastern Monts de Lacaune (including the St. Gervais) and the Albigeois Units (see Guérangé-Lozes and Burg 1990; Doublier et al. 2006)—into the northernmost position. The former nappes of the southern flank of the Zone Axiale follow towards the South.

In the southernmost position, we have placed the protoliths of the Schistes X9 and X15, now preserved in the easternmost part of and at the southern margin of the Zone Axiale (see geol. map sheet 1:50,000 Bédarieux, Bogdanoff et al. 1984). These units contain a conspicuous sequence of (up-section) black meta-cherts, calcite marbles, varicoloured cherts with calc-silicates and dark shales with meta-greywackes. This lithological sequence appears to be unique in the sedimentary record and matches that of the Early Carboniferous on the southern flank of the Zone Axiale (see below). Hence, the Schistes X9 and X15 probably represent a deep part of the tectonic stack of Palaeozoic sediments, and possibly even the autochthonous cover of the Zone Axiale. In the latter case, the Schistes X 1-8 and the gneissic core of the Zone Axiale would represent the original basement to the Schistes X9/15. In the first case, they would have been positioned still south of the Schistes X9/15.

The age of deformation and metamorphism in the Eastern Monts de Lacaune and further to the NW is known

from earlier investigations and new data presented in Doublier et al. (2006). On the southern flank of the Zone Axiale, the age of deformation and metamorphism in the flysch-bearing nappes and their foreland is constrained by the biostratigraphic age of the youngest flysch sediments. The carbonates and plant-bearing clastic sediments of the Namurian A might have been deposited at the front of the advancing nappe stack, i.e., in a "neo-autochthonous" position. Hence, the Viséan/Namurian boundary is the best estimate for the end of marine sedimentation and, therefore, the maximum age of Variscan orogenic deformation. Biostratigraphic data and U–Pb isotopic ages compiled in Weyer and Menning (2006, Fig. 3) reveal that the age of the Viséan/Namurian boundary must be younger than 325 ± 3 Ma, and probably corresponds to an age of ≤320 Ma. Hence, crustal shortening and resulting metamorphism in the flysch bearing nappes and their foreland (Zone Axiale) can only have started in time after 320 Ma.

The accretionary evolution depicted in Fig. 5 also permits to estimate the thickness of the pile of nappes, and, hence, the Variscan burial of the Zone Axiale. Nappes import their maximum metamorphic grade from the basal detachment. Metamorphic grade acquired during D_1/M_1 decreases towards the S, which suggests a rise of the basal detachment in the same direction. This is also indicated by the stratigraphic age of the oldest rocks contained in the nappes, which is Cambrian in the Pardailhan Unit and further North, and Ordovician in the Mont Peyroux and Par-Autochthon Units. In the Eastern Monts de Lacaune Unit, which later came to rest upon the Zone Axiale, maximum metamorphic temperatures were around 300°C (Doublier et al. 2006). With a geothermal gradient of 30°C/km (Doublier et al. 2006), this corresponds to a depth of c. 10 km and a pressure of c. 0.3 GPa. This tectonic overburden was imposed on the hitherto unmetamorphosed foreland sediments (Schistes X9, 15 and sediments positioned further South), when the Eastern Monts de Lacaune and the St. Gervais Unit (the uppermost unit in the roof of the eastern Zone Axiale) were emplaced in their present-day position. Since an autochthonous position of the Schistes X9/15 is not definitely proven, tectonic overburden on the deeper Schistes X and the gneissic core might have been somewhat higher. On the other hand, tectonic overburden might have been even lower, if one considers erosion during nappe transport, or else a higher geothermal gradient.

Extensional and transtensional contacts (D_2 and later)

It appears that the thrust faults which originally separated the nappes have nowhere survived. Although some of the tectonic boundaries between the tectonic units might have originated as D_1 thrusts faults, these boundaries, in their present form, are demonstrably later and relate to extension, partly combined with strike-slip faulting.

The Schistes X4 in the *roof of the Zone Axiale* show intense shearing. Displacement of pegmatites and asymmetric clasts in the Schistes X3 (Vernet orthogneiss) indicate transport top-ENE. Packages within the Schistes X4 contain oblong, ENE-oriented patches of sericite, which suggest retrogression from stretched K-feldspar. These parts of the Schistes X4 represent a major shear zone, which separates the deeper part of the Schistes X from the orthogneiss core and its roof (Schistes X1-3). A more steeply E-dipping, brittle normal fault zone separates the lower Schistes X (4-7) from the higher Schistes X (8-11, see Fig. 2). The highest structural boundary in the roof of the Zone Axiale, the base of the Cambrian St. Gervais Unit, is again more flat (Fig. 2).

It is important to note the outcrop pattern of tectonic contacts at the base and within the Schistes X. The geological maps 1:50,000 and our own observations reveal that all tectonic contacts are refolded by the Rosis synform, which is tight in the West and at deeper levels and becomes increasingly more open eastwards and up-section. At map scale (Fig. 2), this is evident from the progressive narrowing of the synform towards the West.

The *southern margin of the Zone Axiale* is formed by a corridor of steep, ENE-trending faults confined between the orthogneisses and deeper Schistes X to the North and the fossiliferous Palaeozoic rocks to the South (Figs. 2, 6). Reduction of the lithological and metamorphic profile along these faults indicates a component of normal faulting. Previous authors (e.g., Cassard et al. 1993; Echtler 1990; Echtler and Malavieille 1990; Maluski et al. 1991) have interpreted these faults as resulting from dextral transtension. It is agreed, however, that overthrusting of the Schistes X14 over Mesozoic rocks in the area around Bédarieux documents some reactivation by Pyrenean dextral transpression ("faille de Mazamet", Fig. 2, see also Demange 1998; Gèze 1949; Roques 1941).

Unfortunately, the main fault at the southern margin of the Zone Axiale is largely masked by the Jaur and Orb valleys, so that fault kinematics have to be inferred from adjacent rocks of the fault corridor. The following observations indicate a component of dextral shear:

- On the southern flank of the Caroux Antiform, there are frequent indications of ductile dextral shear (see below, chapter on the Zone Axiale).
- The southernmost fault in the ENE-trending corridor swings round to the SSE in the area E of Olargues (Fig. 2). This latter segment has been termed the "queue de cochon" (=pigtail) because of its crooked outcrop pattern caused by erosion. The "queue de cochon" segment is a brittle normal fault with displacement

down to the WSW. It cuts across mesoscopic D_3 fold structures (Aerden 1998) and also truncates the map-scale D_3 structures (Tarassac Synform, Ceps-Le Lau Antiform, Roquebrun Synform; see Fig. 2). Strain compatibility demands that the ENE-trending fault segment is dextral/transtensional.

- The bilateral sense of extensional shear in the Zone Axiale requires accomodation by strike-slip along its margins.

The tectonic *boundary between the Faugères and Mont Peyroux Units* is a key point in the deciphering of tectono-metamorphic events on the S flank of the Zone Axiale. It is a brittle fault with a shear sense top to the E, which is refolded by D_3 (see Figs. 2, 6). It deforms, i.e., post-dates, the dominant slaty cleavage (Fig. 7). This cleavage is identified below (see chapter on mesoscopic structures on the S flank), as S_2. Since the fault affects S_2 and is refolded by D_3, it can be dated as "late D_2". In its northwestern segment N of the village of Ceps, where the Faugères Unit plunges westwards under the Mont Peyroux Unit (Fig. 2), the fault appears as a reverse fault. This is due to refolding about SW-dipping D_3-axes. In fact, the Faugères/Mont Peyroux boundary fault originated as an extensional fault: as demonstrated by Engel et al. (1981; see chapter on very low-grade metamorphism), the fault reduces the zonation of 'illite crystallinity' in the Carboniferous flysch. This demonstrates that the fault is extensional and post-dates the main metamorphism.

Taken altogether, extensional faulting has reduced the tectonic thickness contained between the migmatic gneisses in the core of the Zone Axiale and the highest unit (Pardailhan) to less than 3 km, which highlights the enormous importance of extension.

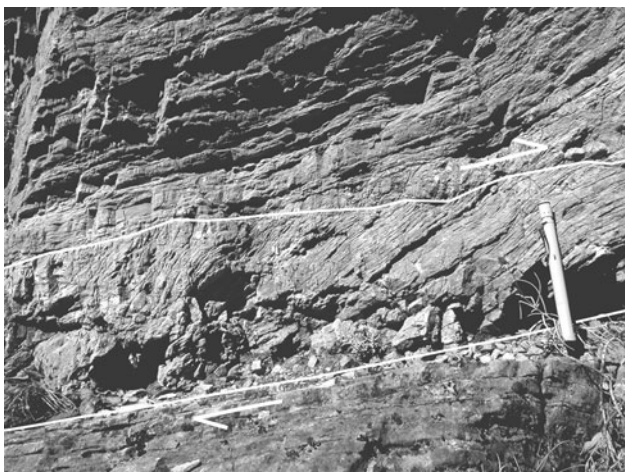

Fig. 7 Top to the E apparent reverse faulting at the boundary between the Mont Peyroux and Faugères Units: small-scale duplex deforming S_2 cleavage. Shear sense top to the right (*East*). Late Devonian griotte limestones SE of Vieussan

Mesoscopic structures and fabrics of the Zone Axiale

The ortho- and paragneisses and the Schistes X show a polyphase deformation described, e.g., by Aerden (1998) and Demange (1998). Folding is especially complex in the highly anisotropic quartzo-pelitic metasediments. The tectonic elements described below can be recognized in most of the outcrops.

The oldest structures are best preserved in paragneisses, or as an internal foliation in competent mineral grains: early folds and foliations represent either some pre-Variscan deformation or else Variscan D_1. In most outcrops, the dominant element is a penetrative foliation at the mm- to cm scale. Some mylonite zones are defined by mm scale foliation and reduction of the feldspar clasts to ≤ 2 mm (e.g., in the Gorges d'Héric 1 km N of the parking). The foliation carries a prominent stretching lineation trending ENE to NE. Although feldspar clasts and quartz lenses are often symmetric, there are frequent foliation-parallel zones with asymmetric clasts and shear bands. While most rocks in the Zone Axiale are SL (plano-linear) tectonites, there are exceptional occurrences of rocks with near-prolate strain. They show pronounced rodding, and the foliation is weakly developed or locally even missing. The best example occurs on the southern flank of the Caroux antiform.

Clasts and shear bands in the orthogneisses and in the roof of the Zone Axiale consistently show transport to the WSW in the western part, and to the ENE in the eastern part of the Zone Axiale (Figs. 1, 8). This bilateral symmetry has already been pointed out in earlier publications (Faure and Cottereau 1988; Mattauer et al. 1996). As laid out in the discussion, this bipolar array is not compatible with D_1 thrusting. Instead, the structural inventory described above reflects the extensional phase D_2.

The excellent outcrops in deeply incised valleys permit to observe that the main foliation with its top-ENE shearing gradually takes on, towards the steep flanks of the dome, the attitude of strike-slip zones, whereby the top ENE shear appears as dextral shear on the N flank and sinistral shear on the S flank.

An exception is observed at the southern flank of the Caroux Dome. In this area, orthogneisses show not only the sinistral shear (resulting from folding of top-ENE shearing), but also intermittent foliation packages with a dextral shear sense recorded by well-developed asymmetric clasts (Fig. 9a), by local drag folds with subvertical axes (Fig. 9b), and by the offset of pegmatite veins. Since the planes with opposed shear senses are more or less parallel, there are no recognizable overprinting relations. The frequency of dextral shear zones decreases towards the North. Deformed pegmatites cutting across the main foliation have, so far, only revealed dextral shear on the foliation.

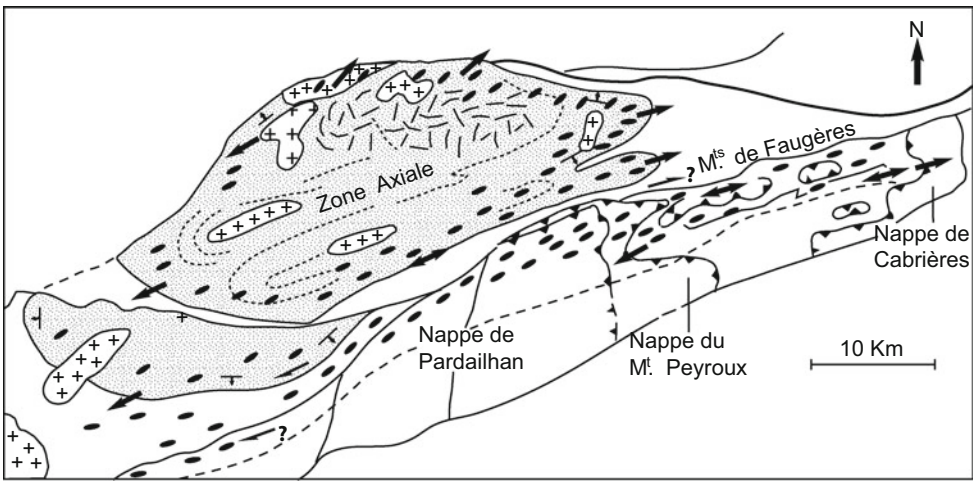

Fig. 8 Diagrammatic representation of the X-axis of the strain ellipsoid and sense of ductile shear in the Zone Axiale and adjacent parts of the southern nappes (redrawn after Mattauer et al. 1996)

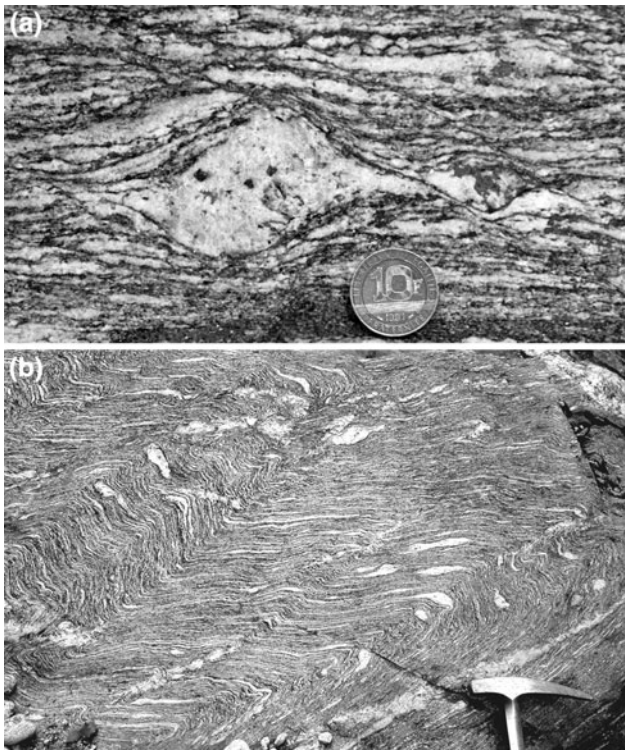

Fig. 9 **a** Dextral sigma clast and shear bands in orthogneiss. Southern flank of the Caroux dome, Gorges d′Héric, 200 m N of Pont des Soupirs. **b** Late dextral shear folds with steep axes deforming the main foliation in gneiss with deformed granite veinlets. Southern flank of the Caroux dome, Gorges d′Héric, **c** 500 m N of Pont des Soupirs. The figured surface is subhorizontal

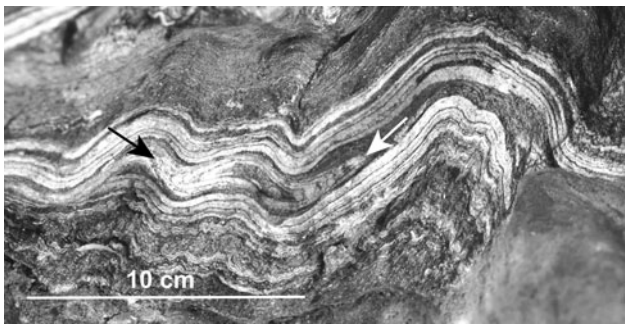

Fig. 10 Approx. NS-directed section across non-cylindrical fold (see *arrows* pointing at hinges), intra-folial in S_{2a}, refolded by late open folds with subvertical crenulation cleavage. Schistes X7, Caroux dome E of Croix de Combes. Specimen: courtesy J. Hormann

This suggests that the dextral post-dates the sinistral shearing. The dextral movements probably reflect shear sense on the southern boundary fault of the Zone Axiale, which post-dates the main deformation of the gneissic core.

Locally, the main foliation has been refolded into non-cylindrical folds whose X-axis parallels the stretching lineation on the main foliation (Fig. 10). As observed by Aerden (1998), the dominant system of folds affecting the main foliation is grossly upright and ranges from the large-scale Espinouse and Caroux Domes (Fig. 3) down to the mm/cm-scale (Fig. 10). Subordinate folds show opposed asymmetries on the flanks of major structures. In the gneisses and intercalated metasediments, fold axes show a uniform shallow plunge toward the ENE. The opening angles of the folds vary between $\geq 90°$ in coarse-grained orthogneisses and near-isoclinal in less competent rocks. In well-foliated rocks, folding is accompanied by mm- to cm-scale crenulation. Since the quartz fabric has been annealed by late thermal overprints, axial plane cleavage is not very pronounced and, in many cases, only detectable from oriented micas observed in thin section. It is important to state that the orientation of stretching lineation, fold axes and crenulation may vary within narrow limits from one place to another, but are strictly parallel with each other within the individual foliation packages (Figs. 11a, b).

A still younger fabric developed in the gneisses is a subhorizontal spaced cleavage indicating vertical shortening (Fig. 12; see also Aerden 1998). The orientation of the

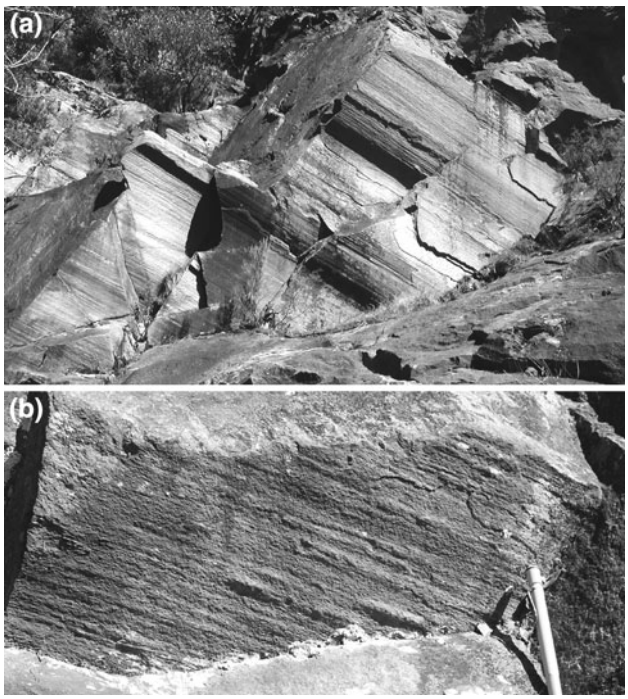

Fig. 11 **a** Strict parallelism of open D_2 folds with L_{2a} stretching and L_{2b} crenulation lineations. N flank of the Caroux antiform. Gorges d′Heric. **b** L_{2a} Stretching lineation parallels L_{2b} crenulation lineation. Detail of Fig. 11a

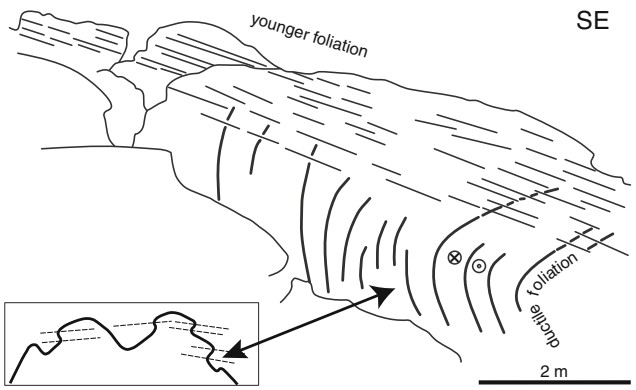

Fig. 12 Brittle foliation formed during vertical shortening transsects earlier, ductile S_{2a} foliation. Orthogneisses, W of Moulin de la Fage (NE part of Caroux Dome). *Inset* diagrammatic representation of late vertical shortening overprinting compression

fold axes is variable, since it depends on the orientation of the pre-existing foliation. Brittle normal faults throwing down to the E represent the youngest increment of extension.

Mesoscopic structures and fabrics on the S flank

Structures and fabrics related to the *phase of nappe emplacement (D_1)* are rare. The most important heritage of D_1 is the overturned position of rocks in the Mont Peyroux and parts of the Faugères Units, which represent overturned limbs of D_1 fold nappes. S_1 axial plane cleavage (in the terminology of the present paper) has regionally been transposed by S_2, and only survived in the Roquebrun Synform (Fig. 2). It is almost completely absent from the Carboniferous flysch of the Mont Peyroux Unit, because these rocks represent a very high structural level. D_1 fold hinges are likewise rare, and have mostly been overprinted by D_2 (see below). Only the Ordovician sediments in the Roquebrun Synform show tight D_1 folds, which trend around SW/NE, face toward the SE and were recumbent prior to their refolding by D_3. A km-scale D_1 fold in the Carboniferous flysch of the Mont Peyroux Unit trends NNE and faces toward the ESE (Engel et al. 1981). In some of the hectometric D_2 folds described below, one or more stratigraphic members are missing, and the stratigraphic break has been folded together with the adjacent rocks. These stratigraphic breaks represent refolded D_1 faults.

The dominant deformation on the southern flank of the Montagne Noire occurred during the *phase of extension (D_2)* with southward decreasing intensity. As already noted by Arthaud (1970), the dominant cleavage on the S flank of the Montagne Noire (S_3 of Arthaud) cuts both limbs of the D_1 folds. This has also been observed by Engel et al. (1981) in the Carboniferous flysch of the Mont Peyroux Unit. From the Ceps-Le Lau antiform southwards, towards the northern flank of the Roquebrun synform (Figs. 2, 6), South-dipping slaty cleavage decreases in intensity and gradually passes into a spaced cleavage, which dips to the SSE at a shallower angle than bedding. In competent rocks, cleavage is refracted into a NNW-dipping attitude (Fig. 6).

This foliation (S_{2a} in this paper) bears a stretching lineation (L_{2a}) defined by pressure-shadows around competent objects, or else by the shape of diagenetic limestone nodules, often with goniatite shells in their core. As already observed by Echtler (1990), Lee et al. (1988) and Mattauer et al. (1996), the ENE-trending X-axes of the strain ellipsoid parallel those in the Zone Axiale (see also Arthaud 1970 for orientation on the southern flank). Strain defined by near-spherical objects decreases southwards, away from the Zone Axiale. It is only at the southern margin of the Montagne Noire that the nodules are more or less spherical. In most cases, deformation is plano-linear. Locally, the deformed limestone nodules define a near-prolate strain (Fig. 13a). The aspect ratio X/Z may exceed factor 10. The coarser-grained silica fillings in radiolarians and calcite fillings in goniatite shells provide a competence contrast with the surrounding, finer-grained matrix and occasionally form asymmetric clasts with a sense of shear toward the ENE (Fig. 13b). In more competent rocks such as detrital limestones or slates, there are calcite-filled tension gashes grossly oriented in the YZ plane of the strain ellipsoid (Fig. 14).

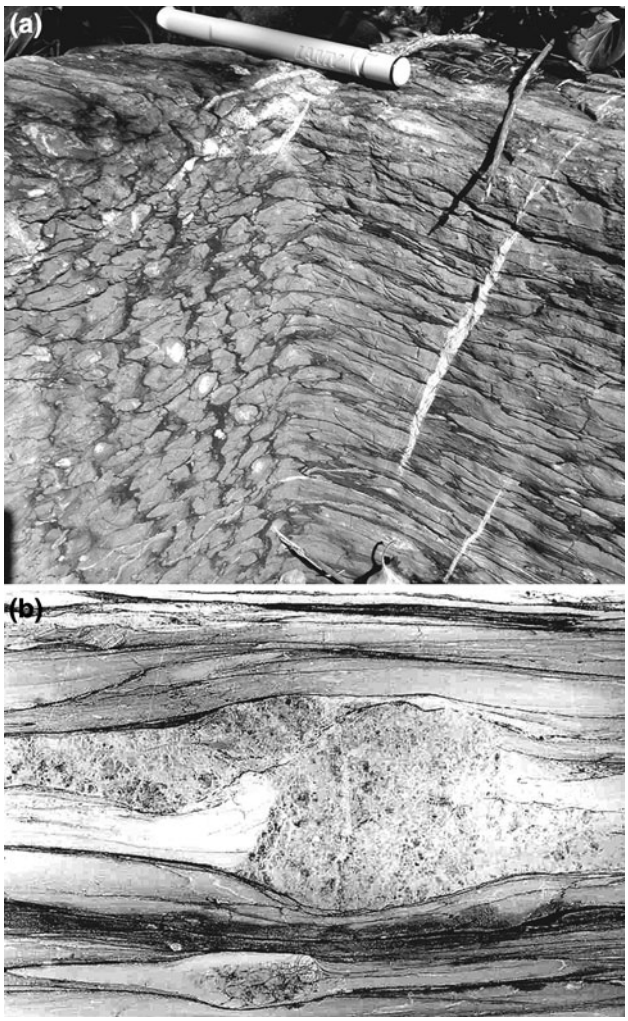

Fig. 13 **a** Stone trough sculpted from Late Devonian nodular limestones ("griotte"). The stonemason has made use of the X-axis of the strain ellipsoid. E of Félines-Minervois. **b** Delta clast formed from a calcite patch (filling of goniatite shell?). Shear sense top-to-the ENE (*right*). Late Devonian griotte limestone, SE of Vieussan (Faugères Unit). Height of clast: 2 cm

Slaty cleavage in metapelites is overprinted by a well-developed crenulation with a wavelength usually below 1 mm. The crenulation lineation (L_{2b}) trends ENE. The axial planes to the crenulation are marked by a spaced crenulation cleavage (S_{2b}) which forms large angles with S_{2a} and has been refolded, together with S_{2a}, by the late open D_3 folds (see below, Fig. 21). Therefore, the crenulation cleavage must be interpreted as a late increment of D_2. The crenulation lineation L_{2b} is exactly parallel with the stretching lineation L_{2a}. We have not observed overprinting relationships. Besides, the calcite-fillings of tension gashes (perpendicular with the stretching lineation) form casts of the crenulation in the encasing slates (Fig. 14). This demonstrates that, at the time of extensional failure, crenulation was already present. It is self-evident that every single extensional surface can only be folded

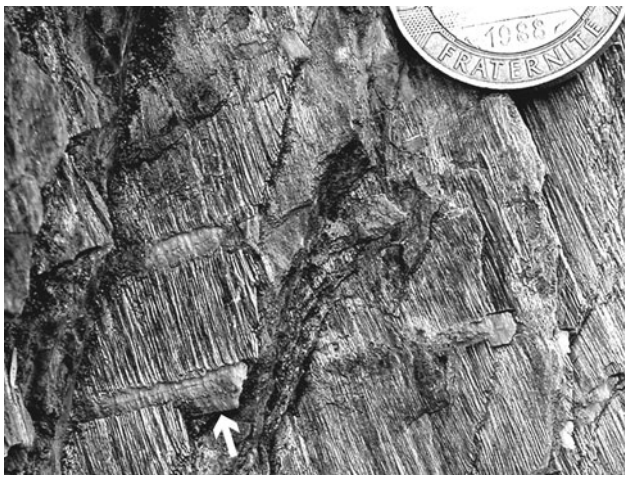

Fig. 14 Calcite-filled tension gashes in slates, grossly perpendicular with L_{2b} crenulation (and L_{2a} stretching lineation in neighbouring rocks). Note that the calcite forms casts of the crenulation (*arrow*). Down = SW. Mid-Viséan limestone-shale sequence, Faugères Unit. Moulin de Graïs S of Vieussan

after its formation. However, the features described above indicate that shortening in NNW and extension in ENE overlap in time and on the regional scale. Therefore, S_{2a} and S_{2b}/L_{2b} have been grouped together within one complex D_2 deformation phase.

The highly anisotropic sequences of the late Devonian to middle Viséan (nodular limestones, shale and cherts) show self-similar folds with wavelengths varying between cm and km scale. In the northern part of the Orb Valley, as far south as the village of Ceps, these folds are tight to near-isoclinal. In most folds, there is a complete stratigraphic sequence, although the thickness of individual stratigraphic members may be reduced, in the fold limbs, to 10% and even less. This indicates that, under the P/T regime prevailing, these stratigraphic members had very similar rheological properties so that folding was harmonic. The axial planes of the folds are parallel with the dominant slaty cleavage. In the zones of highest strain, i.e., in nodular limestones and radiolarian cherts, the fold axes are often sub-parallel with the stretching lineation. However, there is a large dispersal of fold axes on the cleavage plane (see also Arthaud 1969). In three-dimensional outcrops, fold axes are always seen to be curved. Evidently, the dispersal of the fold axes (Fig. 15) represents non-cylindrical folds, although exposed examples are very rare (Figs. 16a, b). The sharpest curvature of the fold axes occur in fine-grained limestones intercalated among shales and cherts. In the more competent Carboniferous greywackes and Ordovician sandstones, folds are also non-cylindrical, but the curvature of the fold axes is less tight (Fig. 16 b). The more massive limestones of the Early and Middle Devonian exhibit only large-scale folds (see below). The early

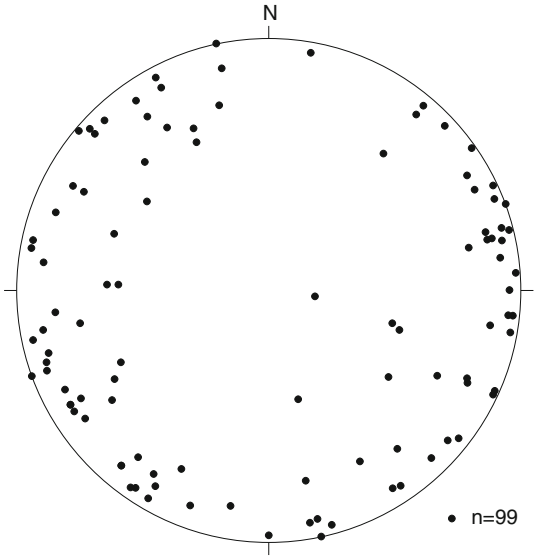

Fig. 15 Dispersal of D_2 fold axes in Late Viséan greywackes of the Faugères Unit. Equal area projection, lower hemisphere

diagenetic dolomites at the base of the Devonian do not show any folding, but brittle structures (Fig. 17).

The direction of younging in the "noses" of the non-cylindrical folds appears to depend on the prevalent orientation of sedimentary bedding (normal or inverted): in inverted limbs (probably formed during D_1), younging is toward the WSW (as in the diagrammatic representation of Fig. 17), whereas it is toward the ENE in normal limbs. From these relationships, we infer that the non-cylindrical folds were imposed on earlier recumbent folds and reflect shearing towards the ENE.

Detailed mapping has revealed that folds of hectometric to kilometric scales very often show opposed directions of younging in the hinges: folds facing to the South have been interpreted, by earlier authors, as auxiliary folds relating to large D_1 folds (e.g., Arthaud 1970). However, folds facing to the North are likewise important (Fig. 18). These opposed facing directions can be shown to have formed in two different ways, although distinction between these two options is often hampered by erosion or insufficient outcrop.

- Refolded D_1 folds have been identified in places where they were rotated, during D_2, into a subvertical position, i.e., into the field of finite D_2 shortening. In these cases, S_2 slaty cleavage cuts across the axial planes of earlier folds (Fig. 19a, b), and the newly formed D_2 folds show opposed facing (Fig. 19b). Mesoscopic D_1 folds with axial planes in the field of finite D_2 extension have not been identified, probably because they were completely transposed.
- Alternatively, opposed facing may represent the flanks of large non-cylindrical folds or even sheath folds. The best map-scale example is represented in Fig. 20, where a synform and an antiform with opposed facing directions merge with each other into an ellipsoidal outcrop pattern. The axes of the syn- and antiform parallel the stretching lineation. The overall structure is that of a flat tube with the long axis plunging toward the WSW.

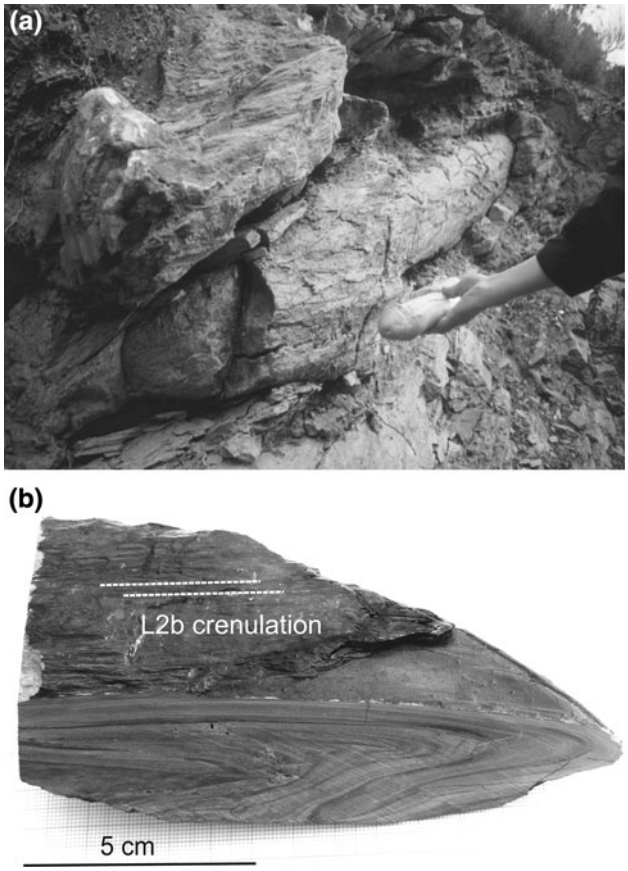

Fig. 16 **a** ENE-trending sheath fold in mid-Viséan limestone-shale sequence, in the core of a kilometric fold structure. Direction of younging is toward the left (WSW). French "flute" bread loaf for scale. Faugères Unit, road Le Pin—Le Lau. **b** Non-cylindrical fold in Viséan flysch with L_{2a} stretching lineation and L_{2b} crenulation lineation and perpendicular tension gashes. Faugères Unit. Road S of Aigues-Vives

Anyhow, all the D_2 folds described above change southwards, along with the decreasing intensity of S_{2a} cleavage, in that the opening angle increases, the curvature of the fold axes decreases, and the folds permit to recognize southerly vergence. As already described by Arthaud (1970: D_3, S_3) these South-vergeing folds and the associated cleavage post-date the recumbent fold nappes (D_1).

D_3 deformation refolds all earlier structures and fabrics east of the queue de cochon. Figure 21 shows D_3 refolding of the S_{2a} slaty cleavage and S_{2b} crenulation cleavage. D_3 folds trend 60–70°E and the map-scale folds abut against the southern margin of the Zone Axiale at an acute angle.

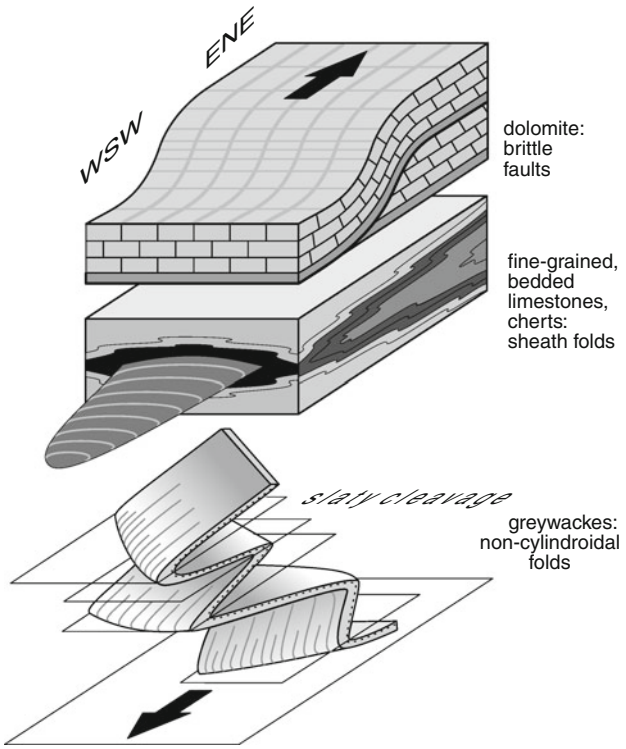

Fig. 17 Diagrammatic representation of D_2 deformation styles controlled by lithology. Highest ductile strain in fine-grained carbonates and radiolarian cherts

The folds are upright and open and range in size from metre- to map-scale. The fold axes plunge towards the SW. Towards the North, the intensity of D_3 increases and an axial plane crenulation cleavage may be developed (see already Arthaud 1970).

Locally, there occur NW-trending, decimetre to metre-scale, open chevron folds or kink folds which deform the S_{2a} cleavage and, hence, must represent a late phase of folding. Their axial planes include large angles with S_{2a}. Since they have only been observed on the NW flank of the D_3 Vieussan antiform, their age relationships with D_3 (as well as with post-D_3 structures) remain uncertain. These folds are not represented in the structural scheme of Fig. 4.

Very low-grade metamorphism (conodont alteration index and 'illite crystallinity')

Very low-grade metamorphism on the southern flank of the Montagne Noire is known from studies of the conodont alteration index (CAI) in Devonian carbonates (Wiederer et al. 2002, Fig. 22) and of 'illite crystallinity' in Cambrian through to Carboniferous rocks of the southeastern Montagne Noire (Doublier 2007; Engel et al. 1981, Fig. 23).

Both data sets are consistent with each other and reveal a decrease of metamorphic grade away from the Zone Axiale. The highest CAI values occur in the Parautochthon adjacent to the Zone Axiale, and in the core of the Ceps-Le Lau Antiform. The zonation of both CAI and 'illite crystallinity' cut across the inverted limb of the large recumbent Mont Peyroux fold nappe (D_1), which is exposed in the Roquebrun synform. 'Illite crystallinity' in the Carboniferous flysch E of the synform shows that the metamorphic zonation also transects the axial plane and the upper, normal limb of the D_1 fold nappe. The areas of elevated CAI and 'illite crystallinity' coincide with the areal extent of the S_2 slaty cleavage. These relationships clearly demonstrate that peak metamorphism in most parts of the Montagne Noire post-dates D_1 and correlates with the dominant D_2 deformation (M_2). M_1 metamorphism created during nappe stacking (D_1) has only been detected

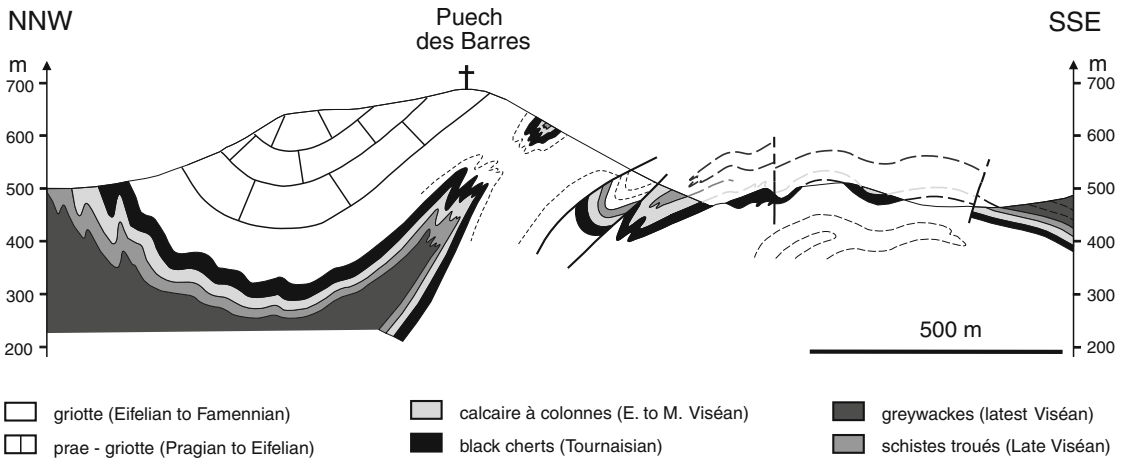

Fig. 18 Tectonic section across the Faugères Unit E of Le Lau (from Doublier 2000)

Fig. 19 **a** Subvertical D_1 folds preserved in steep limbs of D_2 folds, cut by subhorizontal S_2 cleavage. Flysch mudstones of the Mt. Peyroux Unit, Croix de Barrac E of St. Nazaire. **b** Subvertical D_1-folds preserved in steep limbs of D_2 folds, cut by subhorizontal S_{2a} cleavage. Mid-Viséan limestone-shale sequence. Faugères Unit, forest road N of cemetery Le Lau

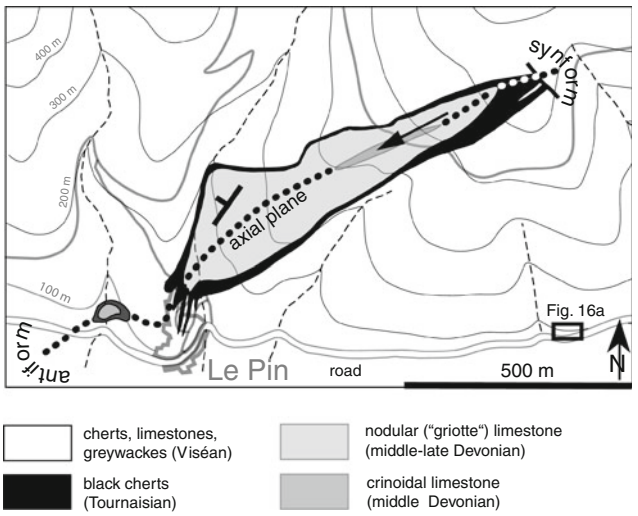

Fig. 20 Kilometer-scale sheath fold in Late Devonian and Early Carboniferous rocks N of Le Pin (Faugères Unit). Curvature of exposure pattern and of the axial plane NW of Le Pin is due to morphology. Note that the southwestern termination to the structure is an antiform, and the northeastern termination a synform (note, in the latter, stratigraphic younging downslope toward the ENE!). Longitudinal fold axis (*black arrow*) plunges more steeply than the slope (i.e., >23°). *Inset* location of sheath fold depicted in Fig. 16a

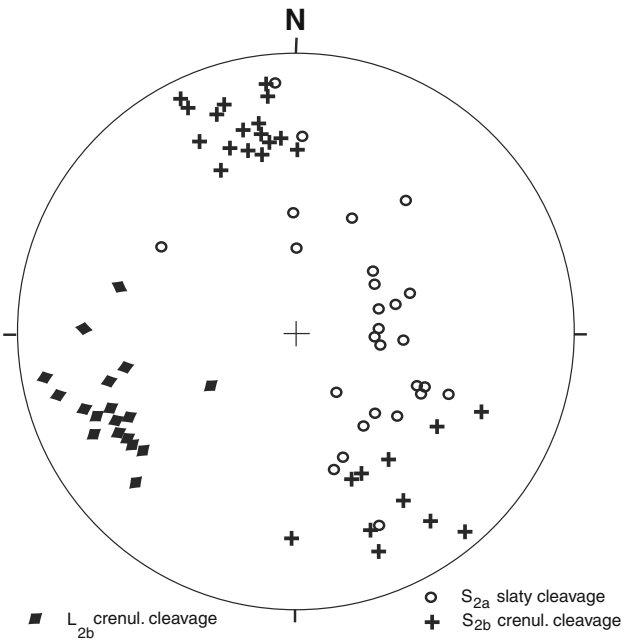

Fig. 21 S_{2a} slaty cleavage and S_{2b} crenulation cleavage both refolded by D_3. S-planes: poles to cleavage planes, equal-area projection, lower hemisphere. Plots are representative measurements from outcrops in the Orb valley, from the N flank of the Roquebrun synform to the N flank of the Vieussan antiform

in western parts of the Pardailhan unit (Doublier 2007) and in the northern flank of the Montagne Noire E of Lacaune (Doublier et al. 2006).

Although tectonic findings reveal formation of the boundary fault after peak metamorphism (late D_2, see above), there is no apparent difference in very low-grade metamorphism between the Faugères and Mont Peyroux Units (Fig. 22). This is possibly due to insufficient resolution of the CAI method. The only major break in the zonation of M_2 occurs in the eastern part of the Carboniferous Mont Peyroux flysch (Fig. 23), where a late normal fault ("secondary" Roquessels fault of Engel et al. 1981) juxtaposes diagenetic grade in the SSE against anchizonal grade in the NNW.

Isotopic ages

U–Pb TIMS datings were carried out by Klama and Dörr at the former Institut für Geowissenschaften of Justus Liebig

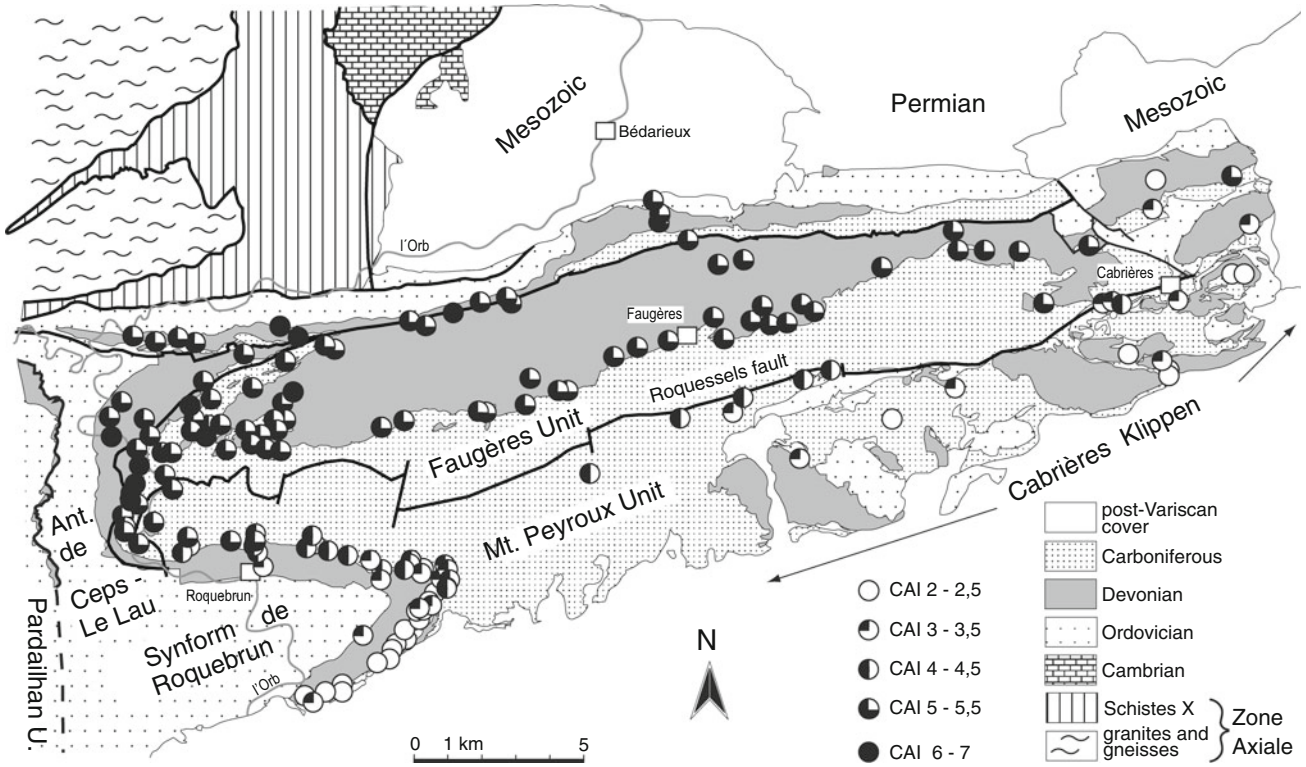

Fig. 22 Distribution of conodont alteration indices (CAI) in Devonian carbonates of the Mont Peyroux and Faugères Units and in the Parautochthon (from Wiederer et al. 2002)

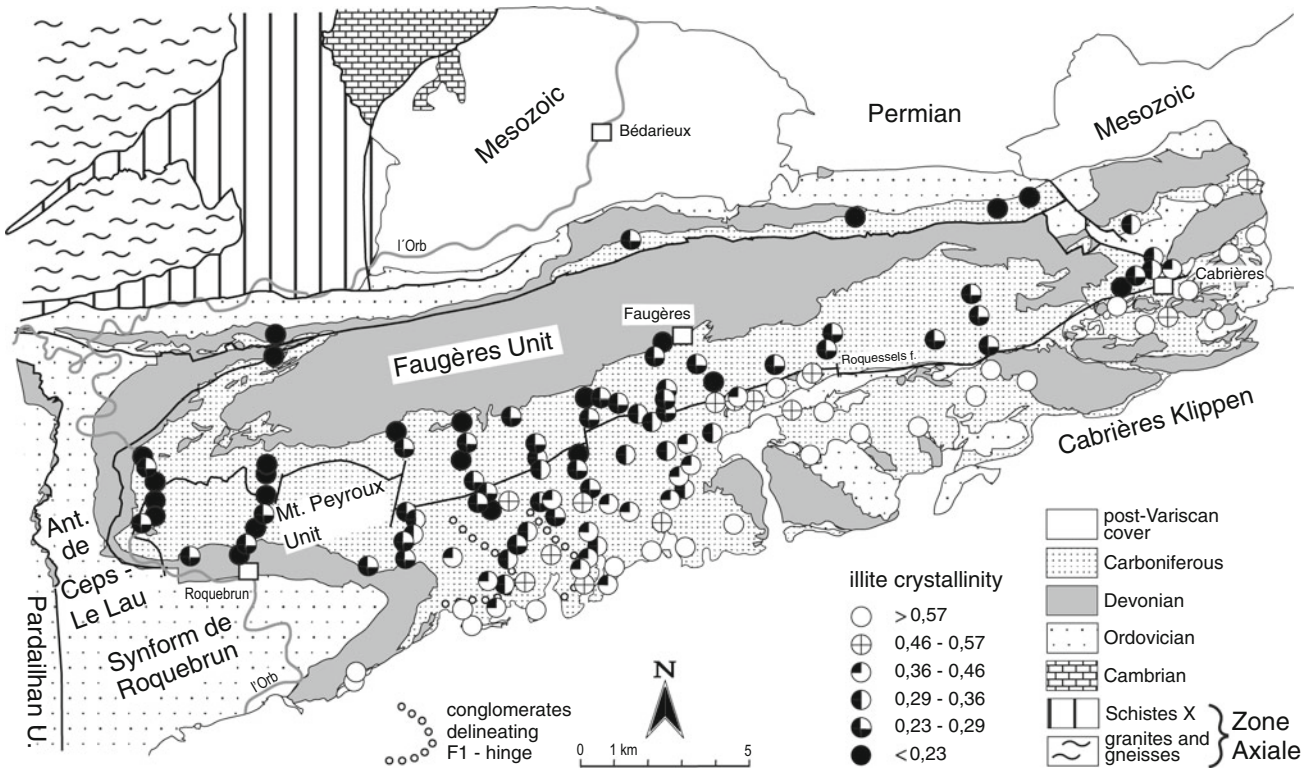

Fig. 23 Distribution of 'illite crystallinity' in the Carboniferous flysch of the Mont Peyroux and Faugères Units (after Engel et al. 1981)

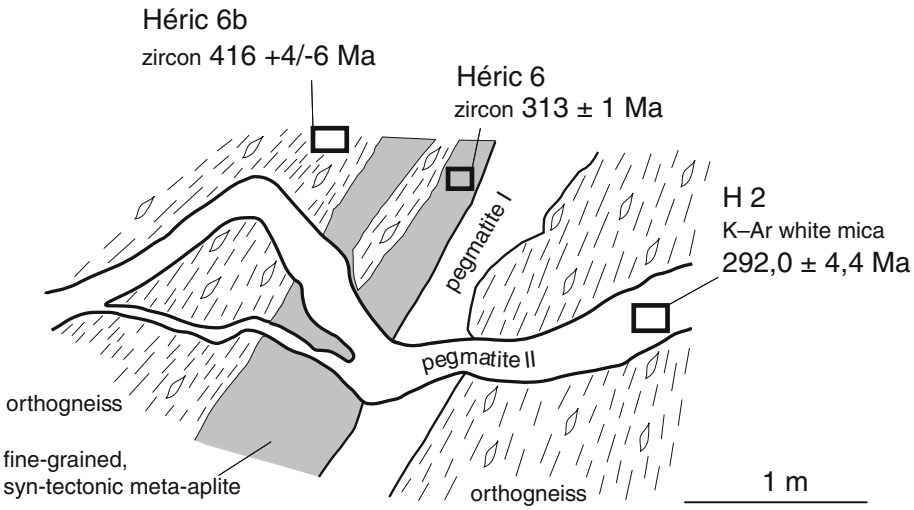

Fig. 24 Foliated orthogneiss intruded by syntectonic fine-grained meta-aplite and an older generation of pegmatite (I), both cut by an undeformed late pegmatite (II). Gorges d′Héric, 450 m N of parking space at entrance to gorges. After Klama (2001)

University Giessen (see also Klama 2001; Klama et al. 2001). Pb and U separation was done using a scale-down version of the ion exchange chemistry for zircon and monazite analyses. Beam intensities allowed static mode measurements using a Finnigan MAT 261 mass spectrometer. The ^{204}Pb was measured with the calibrated ion counter of Spectromat. All isotopic ratios are corrected for mass fractionation (1.12 ± 0.18‰ per a.m.u). The U–Pb data were calculated using PBDAT. Total uncertainties on individual points are represented by 2σ uncertainty ellipses. The datasets were plotted using ISOPLOT. Further details on sample preparation and analytical procedure are given in Dörr et al. (1998) and Dörr et al. (2002).

K–Ar datings on white micas were performed by Wemmer at Geowissenschaftliches Zentrum der Georg August-Universität Göttingen. The analytical procedure is described in Wemmer (1991; see also Doublier et al. 2006).

One key outcrop is situated in the Gorges d′Héric in the ortho-augengneisses of the southern part of the Caroux dome (top. map sheet 1:25,000, 2,543 ouest, St. Gervais-sur-Mare, x 650,800/y 3,142,090, see Fig. 2). The geological situation is depicted in Fig. 24, and the U–Pb ages obtained are given in Table 1.

In the orthogneiss (sample Héric 6b), the zircons show a discordant array with an upper intercept at 1,258 +110/−120 Ma, and a lower intercept at 416 +4/−6 Ma (Fig. 25). We interpret the lower intercept as the minimum age of crystallization of the granitic protolith.

In the same outcrop (Fig. 24), a fine-grained meta-aplite dike (Héric 6) has intruded the orthogneiss subparallel with the foliation, and has, in its turn, been foliated after its crystallization. Hence, the dike is syn-tectonic. It contains quartz, K-spar, plagioclase, biotite and muscovite. One of the analyzed monazites is concordant (Fig. 26). It defines an age of 313 ± 1 Ma which is taken to reflect crystallization of the granite dike. Three zircons define a discordia line (Fig. 27), whose lower intercept (309 ± 3 Ma) matches the concordant monazite within error. The upper intercept (914.4 ± 9 Ma) indicates an inherited component. A monazite isochron plot yields the same age with a larger error bar (313 +7/−5 Ma, Fig. 28). Slightly discordant monazites with $^{207/206}$Pb ages between 328 and 320 Ma are inherited and remind the concordant monazite fraction of 327 ± 4 Ma reported from the Vialais granite in the southeastern part of the Espinouse dome (Matte et al. 1998).

An older generation of pegmatite (adjacent to and parallel with the meta-aplite) has not yielded datable minerals.

The last event recorded in the outcrop of Fig. 24 (sample no. H2) is a younger pegmatite, which crosscuts all other dikes and tectonic fabrics and does not show any deformational features. It contains large crystals of K-spar, quartz, biotite, muscovite and tourmaline together with small pink garnets. A multigrain sample of muscovites has yielded an K–Ar age of 292.0 ± 4.4 Ma (see Table 2).

The second outcrop (near Gouffre du Cérisier in the Gorges d′Héric, top. map sheet 1:25,000, 2,543 ouest, St. Gervais-sur-Mare, x 650,125/y 3,143,150, locality of Fig. 29 in Fig. 2) exposes foliated orthogneiss and foliation-parallel, boudinaged pegmatite truncated by a subvertical dike of apparently undeformed microgranite (sample Héric 2). The granite consists, besides quartz, of perthitic K-spar, plagioclase, muscovite, biotite, green tourmaline, apatite and garnet. Quartz grains show undular extinction and formation of subgrains, but no planar fabric. While 11 zircons turned out to be discordant, a few zircons are near concordia close to 440 Ma (Fig. 30). They have a similar position in the concordia diagram as the discordant zircons from the orthogneiss and suggest that the melt of the granite dike may have been derived from an orthogneiss protolith. A muscovite concentrate from the continuation of the dike on the W bank of the river (sample H3, Table 2) has yielded a K–Ar muscovite age of 294.3 ± 6 Ma.

Table 1 Analytical data of U–Pb datings

Sample	Weight (mg)	Pb (rad.) (ppm)	Pb (ini.) (ppm)	U (ppm)	$^{206}Pb/^{204}Pb$	Radiogenic ratios		$^{207}Pb/^{206}Pb$	Rho	Apparent ages (Ma)		
						$^{206}Pb/^{238}U$	$^{207}Pb/^{235}U$			$^{206}Pb/^{238}U$	$^{207}Pb/^{235}U$	$^{207}Pb/^{206}Pb$
Heric 6 Aplite												
1006 (Mz)	15	620.2	5.96	1,864	990	0.04989 ± 14	0.3678 ± 22	0.05346 ± 28	0.51	314 ± 1	318 ± 2	348 ± 12
1007 (Mz)	17	471.8	3.88	1,245	1,024	0.04978 ± 19	0.3716 ± 24	0.05414 ± 28	0.61	313 ± 1	321 ± 2	377 ± 12
1008 (2 Mz)	18	438.1	3.84	1,162	948	0.04887 ± 23	0.3639 ± 29	0.05401 ± 33	0.62	308 ± 1	315 ± 3	372 ± 14
1010 (Mz)	36	436.9	1.49	1,233	2,607	0.04978 ± 12	0.3658 ± 13	0.05330 ± 14	0.69	313 ± 1	317 ± 1	342 ± 6
1026 (Mz)	11	450.9	1.24	1,182	2,950	0.04901 ± 54	0.3596 ± 44	0.05322 ± 26	0.92	309 ± 3	313 ± 4	343 ± 11
1027 (Mz)	28	313.3	1.52	724	1,502	0.04963 ± 77	0.3707 ± 78	0.05415 ± 74	0.76	312 ± 5	320 ± 7	378 ± 31
1028 (Mz)	**24**	**707.5**	**3.44**	**1,688**	**1,581**	**0.05054 ± 10**	**0.3704 ± 11**	**0.05315 ± 10**	**0.74**	**318 ± 1**	**320 ± 1**	**333 ± 4**
1030 (Mz)	88	445.3	8.23	1,039	415	0.04989 ± 07	0.3732 ± 19	0.05425 ± 25	0.42	314 ± 1	322 ± 2	381 ± 10
1110 (Mz)	10	345.1	2.06	785	1,227	0.05039 ± 23	0.3721 ± 29	0.05356 ± 33	0.61	317 ± 2	321 ± 3	353 ± 14
1112 (2 Mz)	12	125.5	1.10	270	783	0.04959 ± 50	0.3656 ± 76	0.05348 ± 96	0.51	312 ± 3	316 ± 7	349 ± 40
1046 (Zr)*	19	80.42	125	3,041	59	0.02703 ± 149	0.20451 ± 1828	0.05487 ± 469	0.73			
1047 (Zr)*	27	89.73	60.1	2,148	115	0.04329 ± 12	0.31853 ± 1236	0.05337 ± 198	0.62			
1079 (Zr)	**15**	**24.9**	**0.36**	**489**	**4,737**	**0.05478 ± 23**	**0.4171 ± 24**	**0.05523 ± 20**	**0.76**	**344 ± 1**	**354 ± 2**	**422 ± 8**
1080 (Zr)	**10**	**59.7**	**0.43**	**1,267**	**9,148**	**0.04968 ± 15**	**0.3616 ± 16**	**0.05279 ± 17**	**0.68**	**313 ± 1**	**313 ± 1**	**318 ± 7**
1081 (Zr)	10	64.3	6.87	1,418	635	0.04755 ± 13	0.3514 ± 18	0.05359 ± 22	0.57	300 ± 1	306 ± 2	354 ± 9
1082 (Zr)	<10	42.1	5.40	1,030	541	0.04359 ± 17	0.3237 ± 21	0.05384 ± 27	0.65	275 ± 1	285 ± 2	364 ± 11
1083 (Zr)	12	14.9	1.84	276	521	0.05342 ± 47	0.4108 ± 56	0.05578 ± 56	0.67	336 ± 3	350 ± 5	444 ± 22
1126 (Zr)*	10	6.5	1.49	149	305	0.04548 ± 101	0.3709 ± 158	0.05914 ± 207	0.57			
1127 (Zr)	15	40.8	4.13	929	675	0.04642 ± 15	0.3592 ± 29	0.05612 ± 40	0.44	293 ± 1	312 ± 3	457 ± 3
1128 (Zr)*	10	20.9	10.5	685	148	0.03154 ± 28	0.2548 ± 99	0.05859 ± 219	0.26			
1130 (Zr)	<10	31.1	32.4	1,819	76	0.01637 ± 64	0.1706 ± 82	0.07553 ± 201	0.83	105 ± 4	160 ± 8	1,083 ± 29
1131 (Zr)	**14**	**74.6**	**1.06**	**536**	**4,264**	**0.13386 ± 36**	**1.2624 ± 48**	**0.06839 ± 172**	**0.71**	**810 ± 2**	**829 ± 2**	**880 ± 2**
1132 (Zr)*	10	10.6	2.79	256	267	0.04311 ± 58	0.3581 ± 77	0.06024 ± 95	0.67			
Heric 2												
Mikrogranite												
1123 (Zr)	84	35	0.39	496.2	5,729	0.07108 ± 27	0.5521 ± 23	0.05633 ± 10	0.93	443 ± 2	446 ± 2	466 ± 1
1124 (Zr)	<10	9.6	1.1	150.5	625	0.06800 ± 103	0.5469 ± 117	0.05833 ± 83	0.74	424 ± 7	443 ± 9	542 ± 8
1125 (Zr)*	<10	4.9	0.34	106.8	948	0.04735 ± 146	0.4119 ± 203	0.06310 ± 24	0.64			
1134 (Zr)	15	46.5	3.86	386.3	771	0.11978 ± 38	1.9103 ± 77	0.11577 ± 28	0.80	729 ± 2	1,085 ± 4	1,892 ± 5
1135 (Zr)	13	204	7.63	6,681	1,847	0.03317 ± 18	0.2449 ± 15	0.05356 ± 15	0.89	210 ± 1	222.5 ± 1	353 ± 1
1136 (Zr)	23	33.2	0.9	1,089	2,550	0.03324 ± 10	0.2401 ± 98	0.05239 ± 16	0.66	210 ± 1	218.5 ± 1	302 ± 1
1137 (Zr)	24	8.7	0.17	131.9	3,533	0.07060 ± 28	0.5533 ± 45	0.05684 ± 39	0.52	440 ± 2	447 ± 5	485 ± 3
1138 (Zr)	19	16.5	0.78	251.8	1,440	0.07017 ± 40	0.5740 ± 76	0.05932 ± 70	0.44	437 ± 3	461 ± 6	579 ± 7

Table 1 continued

Sample	Weight (mg)	Pb (rad.) (ppm)	Pb (ini.) (ppm)	U (ppm)	$^{206}Pb/^{204}Pb$	Radiogenic ratios		$^{207}Pb/^{206}Pb$	Rho	Apparent ages (Ma)		
						$^{206}Pb/^{238}U$	$^{207}Pb/^{235}U$			$^{206}Pb/^{238}U$	$^{207}Pb/^{235}U$	$^{207}Pb/^{206}Pb$
1142 (Zr)	25	16.4	0.14	232.5	7,906	0.07444 ± 29	0.5945 ± 31	0.05792 ± 23	0.72	463 ± 2	474 ± 3	527 ± 2
1206 (Zr)	8	119.9	3.78	2,002.8	2,179	0.06481 ± 17	0.5132 ± 19	0.05743 ± 15	0.71	405 ± 1	421 ± 11	508 ± 1
1207 (19 Zr)	53	92	5.9	2,403	1,074	0.04159 ± 16	0.3156 ± 15	0.05503 ± 14	0.83	263 ± 1	279 ± 1	414 ± 1
1208 (6 Zr)	15	12.5	0.31	269.4	2,755	0.05018 ± 43	0.3861 ± 53	0.05581 ± 58	0.65	316 ± 3	332 ± 5	445 ± 5
1210 (6 Zr)	33	9.2	0.11	195.5	5,792	0.05064 ± 39	0.3919 ± 39	0.05614 ± 34	0.79	319 ± 3	336 ± 3	458 ± 3
Heric 6b												
Orthogneiss												
1298	12	48.4	0.09	724	10,221	0.06923 ± 21	0.5413 ± 21	0.05670 ± 14	0.76	432 ± 1	439 ± 2	480 ± 6
1300	13	20.8	0.22	318	6,454	0.07025 ± 40	0.5493 ± 46	0.05671 ± 34	0.70	438 ± 2	444 ± 4	481 ± 13
1297	17	33.1	1.2	495	1,845	0.07065 ± 22	0.5601 ± 47	0.05750 ± 44	0.44	440 ± 1	452 ± 3	511 ± 17
1299	31	32.5	2.07	487	1,072	0.07161 ± 14	0.5714 ± 30	0.05787 ± 27	0.44	446 ± 1	459 ± 2	525 ± 10
1295	23	13.1	0.35	189	2,426	0.07242 ± 38	0.5798 ± 49	0.05806 ± 37	0.65	451 ± 2	464 ± 4	532 ± 14
1290	29	13.9	0.71	198	1,300	0.07375 ± 29	0.6011 ± 39	0.05911 ± 30	0.63	459 ± 2	478 ± 4	571 ± 11
	238/204		%	206/204		%						
Heric 6												
Aplite isochron												
1006	19485		11	990		10.8						
1007	20199		15	1,024		14.7						
1008	19028		17	948		17.5						
1110	23997		24	1,227		23.6						
1028	30920		12	1,581		11.8						
1010	51997		23	2,607		22.8						
1026	59825		72.1	2,950		71.6						
1027	29888		116	1,502		114						
1112	15420		37.4	783		36.4						
1030	7947		1.38	415		1.3						

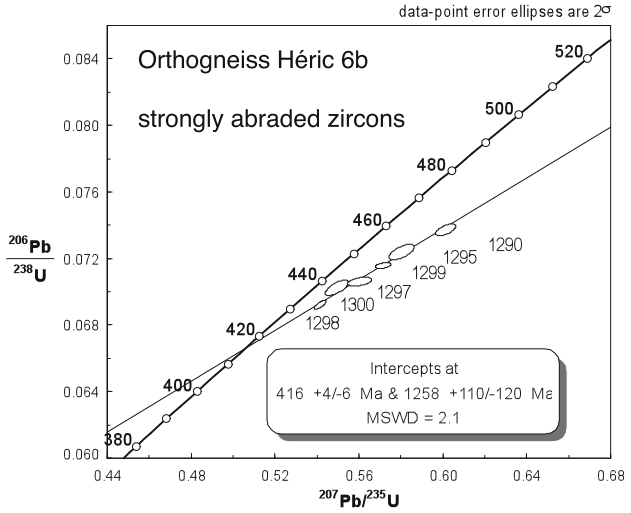

Fig. 25 Orthogneiss sample Heric 6b (see Fig. 24): concordia diagram for strongly abraded zircons

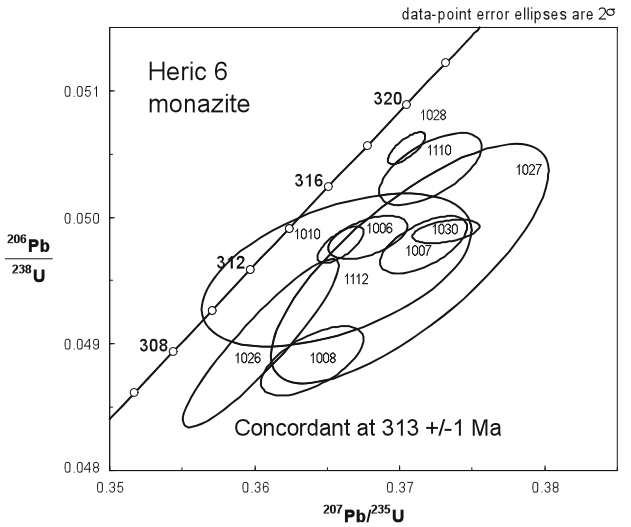

Fig. 26 Fine-grained meta-aplite Heric 6 (see Fig. 24): concordia diagram with plots of single-grain monazite crystals

Further K–Ar muscovite ages around 295 Ma were also derived from other pegmatites at the southern, eastern and northern margins of the gneiss dome (see Fig. 2; Table 2).

- *H1:* NNE-dipping, tourmaline-bearing pegmatite with weakly deformed margins in the southermost part of the orthogneisses, c. 50 m S of the "pont des soupirs" in the E flank of the Gorges d'Héric valley, c. 10 m above the river bed (top. map sheet 1:25,000, 2,543 ouest, St. Gervais-sur-Mare, x 650,925/y 3,141,925; French geodetic system, Lambert zone II). K–Ar muscovite: *293.3 ± 3 Ma.*

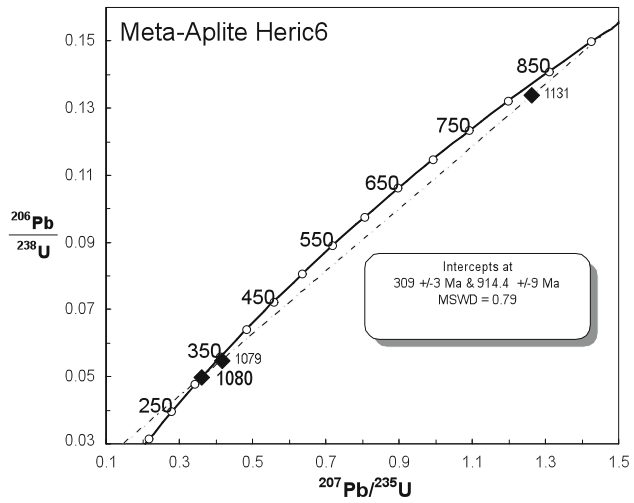

Fig. 27 Fine-grained meta-aplite Heric 6 (see Fig. 24): concordia diagram with discordia defined by three zircon grains

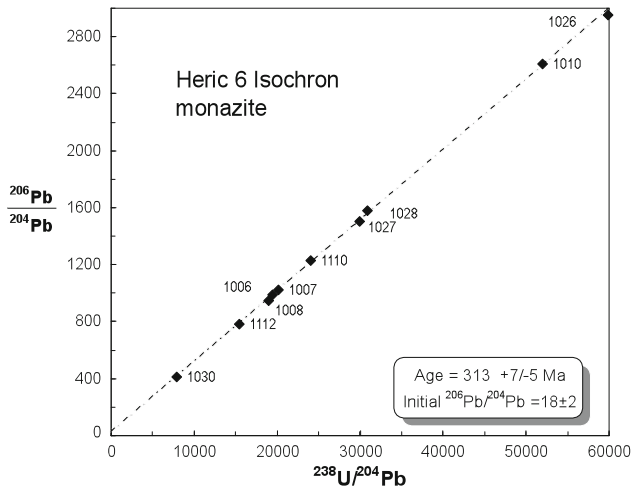

Fig. 28 Fine-grained meta-aplite Heric 6 (see Fig. 24): monazite isochron plot

- *BR 4:* NNE-dipping pegmatite, closely adjacent to or part of the H1 pegmatite; river bed W of and below H1. K–Ar muscovite: *297.2 ± 5.3 Ma*
- *BR 19:* Large pegmatite in the Gorges de Colombières river bed, c. 200 m N of the parking space (top. map sheet 1:25,000, 2,543 ouest, St. Gervais-sur-Mare, x 654,500/y 3,142,850). K–Ar muscovite: *295.2 ± 3.8 Ma*
- *BR 20*: E-dipping pegmatite within Schistes X 3-5, dismembered by top-E extensional shearing, 500 m NE of Rosis (top. map sheet 1:25,000, 2,543 ouest, St. Gervais-sur-Mare, x 654,375/y 3,147,475). K–Ar muscovite: *293.9 ± 6.8 Ma*

K–Ar ages around 295 Ma are not restricted to pegmatites and granites, but occur also in gneisses at the northern margin of the Zone Axiale. A sheet of migmatic

Table 2 Analytical data of K–Ar datings

Sample No.	Rock type	Mineral and grain size	K_2O	^{40}Ar (ng/l)	^{40}Ar (%)	Age	Error 2 s (Ma)
H1	Pegmatite, weakly deformed	Muscovite, large flakes	10.44	107.24	96.60	**293.3**	±3.0
H2	Pegmatite, undeformed	Muscovite, large flakes	10.42	106.70	95.09	**292.0**	±4.4
H3	Granite, undeformed	Muscovite, 2–3 mm	10.41	107.31	98.61	**294.3**	±6.0
BR 4	Pegmatite, weakly deformed	Muscovite, large flakes	10.23	106.59	96.64	**297.2**	±5.3
Do 209	Migmatic orthogneiss	Muscovite, small	10.57	108.97	96.68	**294.3**	±5.8
BR 19	Pegmatite	Muscovite, large flakes	10.33	106.83	95.82	**295.2**	±3.8
BR 20	Pegmatite, sheared	Muscovite, large flakes	10.17	104.68	96.51	**293.9**	±6.8

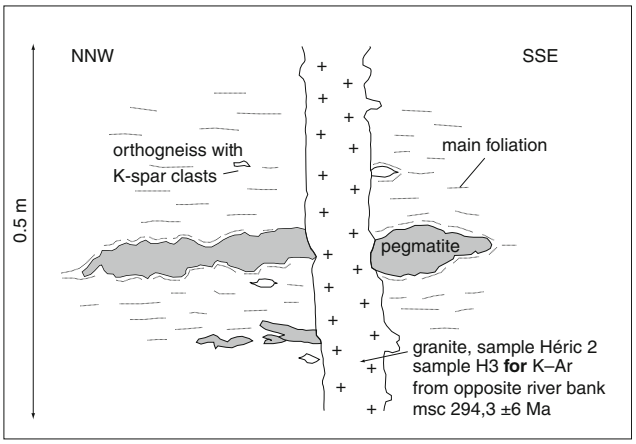

Fig. 29 Subvertical dike of undeformed granite, cutting foliated augengneiss and boudinaged pegmatite. Gorges d′Héric, Gouffre du Cérisier, 1 km N of parking space at entrance to gorges. After Klama (2001)

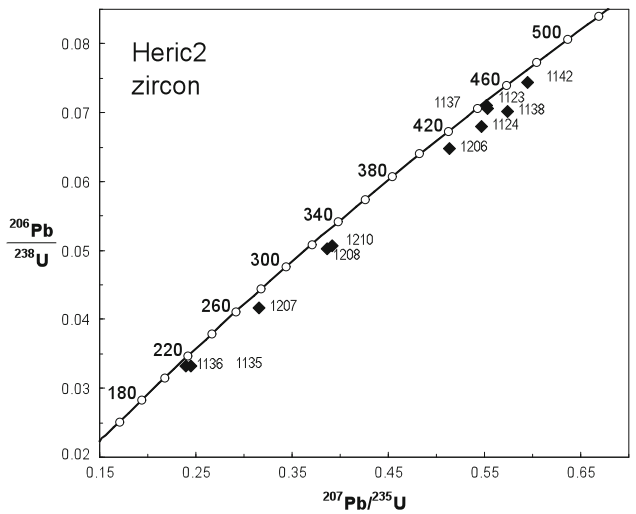

Fig. 30 Undeformed granite dike N of Gouffre du cérisier, Gorges d′Héric: concordia diagram for discordant array of zircon grains

orthogneiss within metasediments contains muscovite dated at *294.3 ± 5.8 Ma.* (loc. see Fig. 1, sample *Do 209*; top. Map sheet 4,243 est, La Salvetat-sur Agout, x 635,100/ y 3,151,975).

Comparisons with similar structural settings

Exhumation of deep-seated rocks by syn- or post-orogenic extension along strike-slip faults is a well-known feature. Prominent examples have been described from the *Alps:* the Tauern Window has been interpreted, by some authors, as an orogen-parallel extensional window which was likewise being shortened during extension (see review and alternative model in Rosenberg et al. 2004). Hot gneiss domes with bipolar extensional shear have also been described from the Aegean extensional belt (e.g., Ring et al. 2004).

Table 3 compiles granitoid ages from the Variscan basement in S-France and northern Spain, which are similar to those obtained in the Montagne Noire. In the *French Massif Central*, there are numerous examples of large granitoid plutons, whose emplacement has been attributed to orogen-parallel extension. These plutonic complexes are (grossly in order from N to S): Guéret, Velay, and the Mont-Lozère-Borne (Talbot et al. 2004), the Aigual, St. Guiral and Liron granites of the southern Cevennes (Brichau et al. 2008) and the Rocles pluton (Be Mezeme et al. 2007). The ages range between 325 and 290 Ma, with the exception of few late Permian microgranite dikes.

In the *Massif de Maures* (Tanneron massif) of southeastern France, Corsini et al. (2004) and Demoux et al. (2008) have described extension-related granites at 320–310 Ma and post-tectonic granites at 303–297 Ma.

A similar age range has been found in the *Pyrenees* (see Gleizes et al. 2006; Maurel et al. 2004; Olivier et al. 2008 and the compilation of Castro et al. 2002). In Table 3, only U–Pb data from this compilation have been listed. They are in general accord with numerous Rb–Sr whole rock ages from the same areas. The tectonic and geodynamic interpretation of the Variscan basement in the Pyrenees is still controversial, although numerous papers invoke transpression (see the discussion in Ábalos et al. 2002). However, one recent study from the Bossòst dome (Mezger and Passchier 2003) reports crustal extension in an overall compressive setting around 305 Ma.

Table 3 Compilation of isotopic ages of granites in regions adjacent to the Montagne Noire

Massif Central			
Guéret Massif (cited after Faure and Pons 1991)			
Brame	324 ± 8	U–Pb zr, mon	Hollinger et al. (1986)
St. Sylvestre	318 ± 5	Rb–Sr WR	Duthou et al. (1984)
Velay dome			
M3 anatexis paragneiss leucosome	314 ± 5	U–Pb abraded mon	Mougeot et al. (1997)
M4 cordierite granite	301 ± 5	U–Pb mon	Mougeot et al. (1997)
Microgranite dikes			Montel et al. (2002)
Montasset	257 ± 8, 306 ± 12	mon el.-microprobe	
Charron	252 ± 11, 291 ± 9	mon el.-microprobe	
Granulite metamorphism at depth	300 ± 20	U–Pb	Pin and Vielzeuf (1983)
Rocles	325 ± 5, 324 ± 4	mon el.-microprobe	Be Mezeme et al. (2007)
Mont Lozère-Borne granodiorite (cited after Talbot et al. 2004)			
Borne	315 ± 5	Rb–Sr WR	Mialhe (1980)
	310 ± 3	Ar/Ar bt	Monié et al. (2000)
Bougès	315 ± 4	U–Pb mon	Monié et al. (2000)
	311 ± 3	Ar/Ar bt	Monié et al. (2000)
Pont-de-Montvert	309 ± 3	Ar/Ar bt	Monié et al. (2000)
Finiels	305 ± 5	U–Pb mon	Monié et al. (2000)
Aigoual-St.Guiral-Liron, Mont Lozère	c. 306	Ar/Ar bt, U–Pb mon, zr	Brichau et al. (2008)
Massif de Maures (Tanneron)			
Migmatite	317-310	U–Pb mon	Demoux et al. (2008)
Migmatization	310, 309	U–Pb mon	Demoux et al. (2008)
	320-315	Ar/Ar ms, U–Pb mon	Corsini et al. (2004)
	Around 300	Ar/Ar ms, U–Pb mon	
Post-tectonic granites	302-297	U–Pb mon	Demoux et al. (2008)
Pyrenees (cited after Castro et al. 2002, Table 8.4)			
Agly deformed granite from core	317 ± 3	U–Pb zr	Olivier et al. (2004)
Agly deformed granite from mantle	307 ± 0.4	U–Pb zr	Olivier et al. (2004)
Ansignan, charnockitic	309 ± 5, 315 ± 5	U–Pb zr	Postaire (1982)
	314 ± 7	U–Pb mon	Respaut and Lancelot (1983)
Saint-Arnac, diorite	308.3 ± 1.2	U–Pb zr	Olivier et al. (2008)
Saint-Arnac, granodiorite	303.6 ± 4.7	U–Pb zr	Olivier et al. (2008)
Bassiès	312 ± 3	U–Pb zr	Paquette et al. (1997)
Quérigut	307 ± 3	U–Pb zr	Roberts et al. (2000)
Mont Louis-Andorra	305 ± 3	U–Pb zr	Romer and Soler (1995)
Mont Louis-Andorra, calc-alkaline	303 ± 3	U–Pb tit	Romer and Soler (1995)
Mont-Louis-Andorra	305 ± 5	U–Pb zr SIMS	Maurel et al. (2004)
	299.8 ± 2.9	Ar/Ar hbl	Maurel et al. (2004)
	292.6 ± 2.8	Ar/Ar bt	Maurel et al. (2004)
Canigou, peraluminous	298, 305	U–Pb mon	Vitrac-Michard and Allègre (1975)
Treilles, charnockitic	293 ± 14	U–Pb zr	Pin (1989)
Bordères-Louron, biotite monzogranite	309 ± 4	U–Pb in situ	Gleizes et al. (2006)

Abbreviations for dated minerals and rocks: *mon* monazite, *ms* muscovite, *tit* titanite, *zr* zircon, *WR* whole-rock

It is also important that HT metamorphism in the Montagne Noire is a really confined to the Zone Axiale and its thermal aureole. Similar thermal anomalies are revealed by the Conodont Alteration Index (CAI) of Palaeozoic sediments in the floor of the *Aquitaine basin* (personal comm. of M. Robardet, Rennes). Likewise, the N-Pyrenean crystalline Trois Seigneurs Massif is situated, in a pre-Alpine reconstruction, westwards and along-strike of the almost unmetamorphosed Palaeozoic rocks of the Mouthoumet Massif (Ábalos et al. 2002). These observations reveal that LP/HT

metamorphism in upper crustal rocks of South France was localized and not regional.

The *Catalan Batholith* S of the Pyrenees has been dated at 296–275 Ma (Rb–Sr, K–Ar and Ar–Ar ages compiled in Castro et al. 2002, Table 8.4., not reproduced in Table 3 of our paper). This age span reminds the young granitoids in the Montagne Noire.

An areally broader perspective has been addressed by Schaltegger (1997), who compiled granitoid geochemistry and isotopic ages from the *Black Forest, Vosges and the External Massifs of the Alps*, i.e., from areas which at least partly represent tectonic equivalents of the French Massif Central. The author defined magmatic pulses at 340–330, 310–307 and 304–295 Ma, which are again very similar to the ages obtained in various parts of France. For the generation of heat and melts, he invoked orogenic processes such as slab detachment or thermal erosion of the base of the lithosphere (see also Faure et al. 2002; Ledru et al. 2001).

The youngest events recorded in the Montagne Noire remind the period of extension and magmatism in the *Southern Alps* between 290 and 275 Ma (Schaltegger and Brack 2007).

Discussion

Kinematic framework

The main phases of the tectonic evolution and their representation in the different tectonic units can be summarized as follows:

D_1: formation and stacking of recumbent fold nappes with tectonic transport towards southerly directions (Arthaud 1970; Echtler 1990; Engel et al. 1981). This process is documented in the eastern Monts de Lacaune (Doublier et al. 2006 and refs. therein), by remnants of recumbent fold nappes and by some refolded folds and faults in the Faugères and lower Mt. Peyroux Units (this paper), and in the Viséan flysch of the eastern Mt. Peyroux Unit (Engel et al. 1981).

It is uncertain, whether the rocks of the Zone Axiale have been deformed during D_1. The main detachment of the accretionary wedge of the Massic Central is situated, in the Montagne Noire, in early Palaeozoic sediments. Hence, the deeper structural levels now exposed in the Zone Axiale might well represent sub-detachment rocks, which escaped from D_1 deformation. The Penninic style nappes inferred by Demange (1998) and minor, pre-D_2 structural relicts could also belong to an older (?Cadomian) orogenic cycle.

D_2: D_2 is the dominant deformation phase and has been formed under the highest temperatures. It is characterized by the main ductile foliation in the Palaeozoic sediments of the southeastern Montagne Noire, where it demonstrably overprints D_1. Ductile foliation, lineation and shear sense in the Zone Axiale matches that in the low-grade rocks, and is, therefore, likewise attributed to D_2.

The kinematic regime of D_2 is clearly revealed by the bipolar array of the shear sense at the opposed ends of the Zone Axiale, which is not compatible with nappe stacking. Instead, the dominant foliation and stretching lineation effect the reduction of the tectonic and metamorphic profile in an extensional tectonic window. As already observed by Echtler and Malavieille (1990) and Nicholas et al. (1977), sense of shear on the northern and southern flanks of the Zone Axiale, combined with transtensional faulting in the eastern termination of the structure indicate a dextral regime. The outline of the Zone Axiale defines a dextral pull-apart structure.

Several lines of evidence indicate that extension in ENE and shortening in NNW largely overlapped in time. Strict parallelism of extensional foliation and lineation with fold axes (in the gneisses) and crenulation (in the Palaeozoic sediments) could be incidental. However, the major D_3 syn- and antiforms become increasingly more open toward the ENE and up-section (Fig. 2). This can only be explained if.

- the active detachment migrated eastwards and up-section, and
- at each extensional surface, NNW-shortening immediately followed upon extension, so that older, initially flat detachment surfaces were progressively folded.

Likewise, the Mt. Peyroux unit was tilted towards the SE ("surdéversement" of Arthaud 1970) before the formation of S_2 cleavage. This tilting can be attributed to contraction in NNW and supports the temporal overlap of D_2 and D_3. This is also indicated, at outcrop scale, by Fig. 14 and the relevant text: extension gashes in the Palaeozoic sediments on the S flank were formed when crenulation was already present. A similar case has been described from the Simplon-Centovalli Fault Zone: it exhumes the metamorphic Lepontine Dome during ongoing shortening (Mancktelow and Pavlis 1994; Keller et al. 2006).

In summary, we propose that the extensional window of the Zone Axiale, during its formation, was being shortened in NNW. Apparently, the Montagne Noire represents a "pinched pull-apart", i.e., an extensional window (extension in ENE) shortened in NNW, generated within an overall regime of dextral transpressive stress (Fig. 31). In this scenario, the various increments of deformation can be interpreted in terms of progressive deformation and uplift of the footwall:

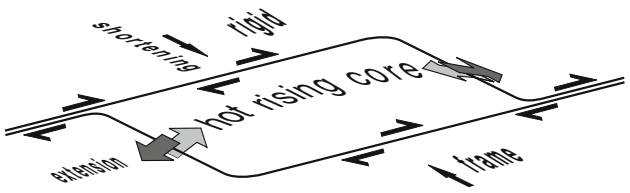

Fig. 31 Deformation model for rocks contained in the pull-apart window of the Zone Axiale: synchronous extension in ENE, vertical shortening and shortening in NNW ("pinched pull-apart"). The governing stress regime is dextral-transpressional

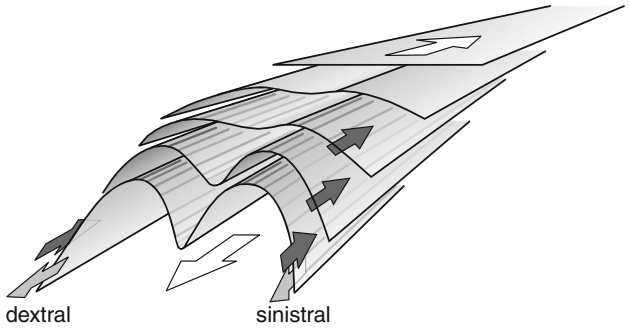

Fig. 32 Model of the structural evolution of the Zone Axiale: extensional shear (top ENE) propagates up-section towards the ENE, and is accompanied by compression in NNW. Folding of detachment surfaces increases with age. Folding effects re-orientation of older, originally flat detachment surfaces into dextral shear on the NNW flank, and sinistral shear on the SSE flank of the Zone Axiale

(a) S_2 extensional foliation, which transposes earlier foliations (Variscan S_1, and older?); formation of a prominent stretching lineation with top-ENE sense of shear.
(b) formation of non-cylindrical folds.
(c) while extension is going on at higher levels: at deeper levels, progressive folding of extensional foliation and non-cylindrical folds into upright folds, with asymmetric second order folds on the flanks.

The combination, during D_2, of shortening in NNW, vertical reduction and ENE extension defines an important component of prolate strain. However, most rocks are SL tectonites, and L-dominated tectonites occur but locally. This contradiction can be resolved, if the plano-linear fabric is explained as a composite foliation (S_2 and earlier), while the L-dominated tectonites represent more competent rocks such as coarse grained orthogneisses and massive nodular limestones which escaped earlier deformation and therefore only record the strain acquired during D_2.

Our results complement earlier findings of Echtler (1990), Lee et al. (1988) and Mattauer et al. (1996), who already pointed out that the stretching lineation in the Palaeozoic metasediments close to the Zone Axiale parallels the trend of the dome. However, these authors have not recognized the largely coeval relationship between extension in ENE with shortening in NNW, the top-ENE sense of shear, and (Lee et al. 1988) the areal extent of the dominant D_2 deformation, whose front actually approaches the southern margin of the Montagne Noire.

Subsequent to ductile D_2 deformation, a brittle extensional fault with transport to the E (late D_2) was formed as the new boundary between the Mont Peyroux and Faugères Units.

D_3 is characterized, on the S flank, by the large-scale, ENE-trending, syn- and antiforms. Their southwesterly plunge can be explained by dextral transpression with transport upwards towards the NW (i.e., at a right angle with the observed fold axes). Mesoscopic folds with a subvertical crenulation cleavage only occur in areas close to the Zone Axiale (Arthaud 1970). D_3 has refolded all ductile and brittle extensional faults. This demonstrates that shortening outlasted extension.

Lastly, the tectonic edifice was affected by the ENE-trending, dextral transtensional faults which, today, delineate the Zone Axiale.

As discussed above, the extensional detachments at the eastern termination of the Montagne Noire propagated upwards/outwards with time, thus enlarging the pull-apart window (Fig. 32). At some stage of the evolution, the extensional window must also have comprised most of the southern flank of the Montagne Noire (including parts of the Pardailhan Unit), which shows largely the same structural inventory as the high-grade core. Today, the southern flank and the core are separated by the bundle of steep dextral transtensional faults, which implies mechanical uncoupling of the formerly coherent structural domains. It appears that the extensional window, at a late stage, was areally reduced to the present-day contours of the Zone Axiale—possibly an effect of cooling and contraction of the isotherms.

Magmatism, metamorphism and isotopic ages

Late Proterozoic and/or Early Cambrian magmatic rocks (around 545 Ma) are widespread in Europe and probably relate to Cadomian activities at the N-Gondwana margin, as already proposed by Cogné (1990). *Ordovician protolith ages* from the orthogneisses of the Zone Axiale may be tied to the sedimentary evolution documented in the Palaeozoic rocks. It is possible that these plutonic rocks have a similar age as the intermediate volcanic rocks intercalated between Caradoc and Arenig sandstones in the Cabrières Klippen. The Ordovician andesites might relate to back-arc extension caused by southward subduction under the N-Gondwana margin. This same process might also account for the late Silurian/early Devonian orthogneiss protolith

dated at 416 +4/−17 Ma (see above). In this scenario, the angular unconformity between the basal Devonian and Cambro-Ordovician in parts of the Montagne Noire can be explained by extensional tilting.

The *first metamorphic event* (or group of events) recorded in the Montagne Noire is pressure-dominated. This cannot be solely explained by Variscan crustal thickening, because the thickness of the orogenic wedge emplaced on the Zone Axiale did not greatly exceed c. 10 km, corresponding to a surplus pressure of 0.3 GPa. Rocks with clearly higher metamorphic pressures described in the previous literature must have been positioned at greater depth already before the arrival of the thrust front.

It is uncertain, whether the local occurrences of eclogite facies metamorphism belong to Variscan stacking (M_1) or to some older event. If they were Variscan, the eclogite protoliths would have been positioned, before the arrival of the nappes, at a depth corresponding to $1.4 - 0.3 = 1.1$ GPa (33 km), i.e., near the base of the crust. The protoliths of the eclogites are ultramafic cumulates, which might well be derived from magmatic underplating before the onset of Variscan orogeny. In this scenario, the U–Pb age of 440 Ma for the eclogites obtained by Gebauer et al. (1988) would not represent HP metamorphism, but rather crystallization of the ultramafic protolith, possibly cogenetic with the intrusion of the orthogneisses and the extrusion of Ordovician volcanics. Equilibration in the eclogite field would have been achieved by the additional load of the nappes. However, these early events (the pre-Variscan state of the lower crust, the age of eclogite metamorphism and Variscan nappe stacking) can hitherto not be tied to any of the available isotopic ages.

The *second phase of metamorphism* (M_2) is characterized by low pressures and high temperatures (see also, e.g., Thompson and Bard 1983), leading to migmatization in the core of the Zone Axiale. The decrease of 'illite crystallinity' and of CAI on the southern flank away from the Zone Axiale, and the array of the metamorphic zonation (cutting across inverted D_1 fold limbs) suggest that very low-grade metamorphism was caused by the rise of the hot Zone Axiale, which effected syntectonic contact metamorphism in the surrounding and overlying rocks.

The *latest increment of LP/HT metamorphism* (M_3 of Doublier et al. 2006) is represented by the thermal overprint on Stephanian coal seams. This event might also account for the Rb–Sr whole rock and mineral isochrons between 290 and 275 Ma in the Sidobre and Folat granites on the N flank of the Montagne Noire (Hamet and Allègre 1976), although these ages are partly at variance with older U–Pb ages from the same rocks (Lévêque 1986). A large-scale thermal event in Stephanian time has also been proposed by Bouchot et al. (1997), Costa (1990) and Van Hinsberg et al. (2007).

Interpretation of isotopic ages requires methodological considerations. While zircon and monazite U/Pb ages are generally accepted as dating directly high temperature events or very early increments of cooling, Ar-ages are supposed to date cooling through closing temperatures well below the crystallization temperature of granitoid melts. Reviews and data by Von Blanckenburg et al. (1989), Villa (1998) and Willigers et al. (2001) give closing temperatures for Ar in muscovite between 410 and 510°C. Such high closing temperatures are especially plausible for large muscovite crystals in pegmatites and granites. In an extensional setting, which favours rapid cooling, K–Ar ages can therefore be expected to be close to the peak temperature of HT metamorphic rocks or the crystallization temperature of granitoid melts.

In the Caroux orthogneiss, Ar–Ar ages on biotite (316 ± 4 Ma; Maluski et al. 1991), as well as the metaaplite dike (313 ± 1 Ma, Fig. 26) are identical within error. The first contact metamorphism of orthogneiss in the Espinouse dome (Krause et al. 2004) has the same age. We also recall here the 314 Ma age of the Folat granite NE of the Zone Axiale (Lévêque 1986). Together, these findings reflect a magmatic event around 315 Ma, which caused heating and subsequent rapid cooling.

The same interpretation applies to micaschists (Schistes X) in the shear zone at the southern boundary of the Zone Axiale, where monazites from an orthogneiss N of St. Pons have yielded a U–Pb age of 308 Ma (Gebauer et al. 1988). Farther E, staurolite schists overlying the same orthogneiss have been dated by Ar–Ar on muscovite and biotite at 311–308 Ma (Maluski et al. 1991). These data suggest a metamorphic event at c. 308 Ma followed by rapid cooling. The latter event and the Roc Noire granite in the Espinouse (Krause et al. 2004) have the same age and demonstrate that the 308 Ma event was also present in the internal (deeper) part of the Zone Axiale.

Our own K–Ar ages and the Ar–Ar ages of Maluski et al. (1991) reveal a cluster at 300–295 Ma, which is present in the uppermost gneisses as well as in the Palaeozoic units, at the southern and northern margins of the Zone Axiale.

The anomalies of very low-grade metamorphism in the Stephanian Graissessac basin either represent a late increment of the 300–295 Ma phase, or else a still younger event.

Taken altogether, our own findings combined with literature data suggest heterochronous magmatism and metamorphism (333, c. 315, c. 308, c. 300 and post-295 Ma) in the relatively small area of the eastern Montagne Noire. Since almost identical age patterns occur also in neighbouring and even in remote areas, it appears that the ages obtained from the Montagne Noire represent areally widespread thermal pulses.

While ages ≥ 330 Ma appear to be restricted to the migmatic core region, the younger ages have been encountered also along the margins of the Zone Axiale and in eastern parts of the Espinouse and Caroux domes. Recognition of an age pattern in the entire Zone Axiale would require much more samples.

The isotopic ages raise a fundamental problem. The oldest monazite age from migmatites and granites in the Espinouse dome range between 333 ± 5 and 327 ± 5 Ma (Be Mezeme 2005; Matte et al. 1998). In the time scale of Weyer and Menning (2006), an age of 333 Ma corresponds to the middle Viséan. At this time, the entire region from the original position of the nappes of the southern flank down to the Pyrenees was an area of marine pelagic sedimentation, which lasted until ≤320 Ma. Therefore, the above monazite ages are not compatible with Variscan crustal thickening and uplift.

Metamorphic ages younger than 320 Ma are likewise incompatible with Variscan thrust loading. The metamorphic and magmatic event at c. 315 Ma post-dates the end of marine sedimentation (≤320 Ma) by ≤5 Ma. This argues against the classical concept of "regional metamorphism" (tectonic stacking followed by thermal relaxation), which leads to peak temperatures only some 15–20 Ma after stacking.

Geodynamic setting

During the last decade, late-orogenic extension, granitoid magmatism and LP metamorphism in the Variscides—including the Montagne Noire—have often been explained by "orogenic collapse", probably triggered by break-off of a subducted mantle slab or a similar process (e.g., Costa and Rey 1995; Gardien et al. 1997; Ledru et al. 2001; Vanderhaege et al. 1999; Vilà et al. 2007). Although heating by rising mantle magmas in a convergent setting is a plausible and powerful process, alternative reasons have been discussed for the derivation of the heat required for crustal melting: radiogenic heat production (e.g., Henk et al. 2000) or viscous heating (e.g., Babeyko et al. 2002; Burg and Gerya 2005).

However, slab break-off and similar processes usually occur during the subduction or early collisional stage of an orogeny, and involve old, cold and dense oceanic lithosphere. Whichever process controlled granitoid magmatism in the Montagne Noire must have affected continental N-Gondwana lithosphere, which underlies the early Palaeozoic shelf sediments. The density contrast between continental lithosphere and asthenospheric mantle is in the order of 0.05 g/cm^3 (Grow and Bowin 1975), which is probably too low to cause detachment.

It is also important to recall that the hot core complex of the Montagne Noire originated in the external part of the orogenic wedge, which evolved from a foreland flysch basin. Nevertheless, extension, LP/HT metamorphism and granitoid intrusions have been as important as in the more internal, northerly parts of the Massif Central. Hence, in the Montagne Noire, crustal thickening and resulting gravitational collapse can be ruled out: collapse of a foreland fold and thrust belt does not exhume rocks of the lower crust.

This aspect is strongly supported by the timing of metamorphism and granitoid magmatism. Collisional deformation between Armorica and Gondwana started at c. 380 Ma (or even earlier, e.g., Matte 1991). Accretion reached the central Pyrenees by the Late Namurian (Engel 1984), i.e., around 315 Ma, and the Basque Pyrenees by the middle Westphalian (Colmenero et al. 2002), i.e., around 312 Ma (timescale of Gradstein et al. 2004). If extension and metamorphism had been related to crustal thickening, extensional exhumation should likewise be diachronous. However, the late-Variscan extensional gneiss domes fall into the same age span (c. 320–300 Ma), from the Northwestern Massif Central down to the Pyrenees. It is also essential to recall here that HT metamorphic pulses in the Montagne Noire both pre-date and post-date Variscan crustal stacking in this area, which rules out models of thermal relaxation after stacking. This consideration supports Brichau et al. (2008), who noted that grantoids dated at 325–305 Ma occur both in northwestern and external (southeastern) parts of the Massif Central, which rules out relationships with prograding orogeny.

Lastly, LP/HT metamorphism in South France is not regionally uniform, but localized. This argues against processes operating uniformly at a large scale. For these reasons, we conclude that heating was independent from Variscan subduction/collision processes. We propose, instead, that metamorphism was caused by the advection of hot, low-viscosity materials (see Franke et al. 2000; Franke 2001), which intruded into a crustal-scale shear zone active from ≥330 Ma onwards, before, during and after tectonic stacking in the Zone Axiale and its surroundings. At least for the time after crustal stacking, structural data reveal a growing pull-apart window, which accommodated the intruding masses. In the early stage of this process, extensional deformation (D_2) had already started and was producing new structures and fabrics, while heating still lagged behind because of the poor thermal conductivity of rocks and because the volume of the heat-advecting intrusives was still small. In this scenario, at least the late part of the medium-pressure metamorphism M_1 coincides with the early part of D_2, which, little later, brought about the high-temperature metamorphism M_2.

The exact nature of the heat-advecting materials remains to be identified: the migmatites and granitoids encountered at the surface might well represent the thermal effects, and

not the causes of HT metamorphism, with the heat source hidden in the subsurface. Anyhow, the negative gravity anomaly coinciding with the Zone Axiale (Corpel et al. 1987) indicates that the intruding materials were felsic. Heat might well have been transferred by dry, overheated felsic melts derived from the lower crust. It is also possible to envisage hot, low-viscosity, felsic solids (gneisses or granulites). A combination of both solids and melts is likewise plausible: uplift of solids may produce melts which enhance buoyancy, either by mere decompression of "dry" materials or else by dehydration of aqueous minerals (e.g., Teyssier and Whitney, 2002). Anyhow, such hot solids, dry melts or granitoids in an orogenic foreland cannot have originated from crustal thickening, but ultimately require heat advection by mafic melts. This mafic heat source must be hidden at deep crustal levels, where it does not affect the local gravity field.

Although geochronological data from the Montagne Noire needs to be complemented, the isotopic ages available suggests heating by separate thermal pulses. This is best explained by repeated rise of hot materials, especially melts. A review by Petford et al. (2000) stresses that granite intrusion operates at timescales of $\leq$100,000 years. Such fast intrusions were probably not only promoted by buoyancy, but also by passive intrusion from deeper levels into the growing pull-apart window. It appears unlikely that episodic and fast intrusive pulses were controlled by magmatic processes in the lower crust or mantle. We suggest, instead, that hot materials were continuously available from $\geq$335 Ma onwards, and that their discontinuous advection was triggered by discontinuous tectonic activities along the dextral master fault system, which provided pathways for the intrusion. Melt migration as a reason for metamorphism has also been discussed in other orogenic belts (e.g., Miyazaki 2004). Melt intrusion may also aid footwall uplift in hot core complexes (Lister and Baldwin 1993).

Comparisons with the Massif Central and Pyrenees reveal that similar thermal anomalies existed over a vast area and during the same time-span. These hot core complexes are probably located in the belt of dextral shear zones, along which Gondwana was displaced westwards with respect to Laurussia during the Permo-Carboniferous, thereby opening the Palaeotethys ocean (Arthaud and Matte 1975). It appears likely that mantle activities responsible for the formation and intrusion of granitoid melts are not related to Variscan collision, but to the westward propagation of Palaeotethys rifting (Franke 2009). Similar processes have been invisaged by Schaltegger and Brack (2007) for the Permian evolution of the southern Alps. In this respect, we also acknowledge the farsighted contribution by Wickham and Oxburgh (1985), who attributed Variscan granitoid magmatism and LP/HT metamorphism in the Pyrenees to crustal thinning in a continental rift or to extensional windows in a strike-slip regime.

The above considerations are quite well compatible with numerical modelling by Rey et al. (2009). These authors found out that far-field tectonic extension provides space for the rise of hot materials, and that heterogeneous bulk pure shear (as it occurs in the Montagne Noire) is favoured by the presence of a molten layer in the lower crust, and a localizing heterogeneity in the upper crust. Such heterogeneity is provided by the massive body of Silurian orthogneiss, which occupies much of the Zone Axiale.

As laid out above, the oldest monazite ages at c. 333 Ma coincide with marine sedimentation documented in the nappes of the southern flank of the Montagne Noire. In the summary by Weyer and Menning (2006), tuffs from mid-Viséan light-coloured cherts in the Rhenohercynian belt have yielded U–Pb zircon ages of 334 and 336 Ma. These cherts occur also in the Montagne Noire. It is interesting to note that this stratigraphic level as well as the overlying "schistes troués" contain widespread limestone turbidites, debris flows with limestone clasts and coeval platform carbonates (e.g., Engel et al. 1981). It appears possible that these shallow water carbonates and their debris originated at compressional highs located in the same strike slip fault system one of which also controlled the opening of the extensional window of the Zone Axiale.

Our model for the Montagne Noire integrates observations and concepts published by previous authors. Arthaud (1970), Demange (1998), Matte et al. (1998) and Soula et al. (2001) have correctly pointed out that compressional strain played a role for the origin of the Zone Axiale. Schuiling and de Widt (1962) and Faure and Cottereau (1988) have invoked diapirism, a process also addressed by Soula et al. (2001). From these papers, our model differs in that we propose a combination of extension in ENE and shortening in NNW, and intrusion of melts or upward material flow of hot, low-viscosity solids, enhanced by the opening of a pull-apart structure. The most recent tectonic model (Charles et al. 2009) invokes nappe stacking and HT metamorphism at 340–325 Ma, followed by diapiric rise of the hot core until c. 325–310 Ma and a final extensional event at c. 300 Ma. This model is invalidated by the timing of processes laid out above, which demonstrates high-grade metamorphism well before the arrival of the nappes and ductile extension already in time before c. 315 Ma. However, the fanning out of stretching lineations (Mattauer et al. 1996) and AMS lineations (Charles et al. 2009) in northern and eastern parts of the Zone Axiale is well compatible with a diapiric component in this area, notwithstanding strike slip-related extension as the regional driving force.

Several recent models have correctly pointed out that extension was the main factor for the exhumation of the Zone Axiale. Van den Driessche and Brun (1989, 1992) have compared the Zone Axiale with asymmetric extensional belts in the Basin and Range province of the USA, with only one extensional shear zone at the northeastern termination of the Montagne Noire, and exhumation in a "roll-under" structure. Our model differs from classical extensional settings of the Basin and Range type in that the latter exhume only rocks metamorphosed at an earlier time. In the Montagne Noire, peak metamorphism still continued during the extensional process, which created the space for the intrusion of melts and/or vertical material flow of low-viscosity solids. In such a scenario, the rising lower plate continues to be heated by the rising hot materials. Pervasive cooling does not start before the hot lower plate approaches the upper crust.

Echtler (1990) and Echtler and Malavieille (1990) have correctly pointed out that extension was bilateral, with top to the WSW movements at the western and ENE-directed shear at the eastern termination of the Zone Axiale. These authors were also the first to describe the kinematic framework of the Zone Axiale with two dextral strike-slip faults at the northern and southern margins and extension at the western and eastern terminations (the pull-apart structure described in our paper). Both Van den Driessche and Brun (1989, 1992) and Echtler and Malavieille (1990) have not integrated, into their model, NNW-directed shortening. One of the novel aspects of our concept is the combination of both shortening and extension in the "pinched pull-apart". It must be noted, in this respect, that at least an alternation of shortening at deeper levels and extensional collapse in the upper crust has been proposed by Aerden (1998) and Aerden and Malavieille (1999).

None of the previous models has considered the problem of timing. Matte et al. (1998) have published an isotopic age for a supposedly post-orogenic granite which, in fact, pre-dates the termination of flysch sedimentation and, hence, the subsequent crustal stacking. This apparent contradiction has been the starting point for our study and represents an important element of the model presented above.

Conclusions

- The gneiss dome of the Montagne Noire (Zone Axiale) rises from under very low-grade Palaeozoic sediments in the external part of the Variscan belt of France. Evaluation of structural, isotopic and biostratigraphic data reveals a grossly southward prograding fold and thrust belt (D_1). The Variscan nappe pile reached the area of the present-day Zone Axiale after the termination of flysch sedimentation (i.e., in time after c. 320 Ma) and added a tectonic thickness of c. 10 km (0.3 GPa).
- Variscan D_1 is mainly documented by extensive overturned sequences which represent inverted limbs of originally recumbent fold nappes. Otherwise, structures and fabrics are strongly overprinted by D_2.
- It cannot be excluded that relicts of pressure-dominated metamorphic mineral assemblages are due to nappe stacking and represent Variscan M_1 metamorphism. Local occurrences of eclogite may also belong to M_1, but could be older. Anyhow, pressure-dominated rocks with pressures well in excess of 0.3 Gpa must have been at deeper levels of the foreland crust already before the arrival of the nappe stack and record some pre-M_1 metamorphism. This pre-M_1 increment either relates to an early phase of strike-slip deformation, or else represents a pre-Palaeozoic (?Cadomian) metamorphic event. The absolute ages of Variscan M_1 and earlier events in the Zone Axiale are hitherto unknown.
- Exhumation of high-grade metamorphic rocks in the Zone Axiale (D_2) occurred in an extensional window provided by a pull-apart structure located at a crustal-scale, ENE-trending, dextral strike slip fault. At an early stage of the extensional process, the extensional window comprised not only the crystalline Zone Axiale, but also important parts of the Palaeozoic mantle on its flanks, which largely reveals the same tectonic evolution. Since extension in ENE was accompanied by shortening in NNW ("pinched pull-apart"), bulk D_2 deformation was in the prolate field. This strain increment is only documented in portions of rock which had remained undeformed during the preceding period of crustal stacking.
- The dominant metamorphism of the Montagne Noire (M_2) is polyphase and occurred under low-pressure/high-temperature conditions. It is closely associated, in space and time, with the extensional deformation (D_2).
- The timing of M_2 metamorphism strongly suggests that heating was independent from the collisional process: the first monazite ages occur at 333 Ma, i.e., are coeval with mid-Viséan sedimentation. Another group of isotopic ages for M_2 occurs around 316 Ma, thus post-dating the end of marine sedimentation by only $\leq$4 Ma. These findings rule out metamorphism by thermal relaxation after tectonic stacking. HT metamorphism and pulses of granitoid intrusions continued around 308 and 300 Ma. A still younger event between in or after Stephanian time (M_3, $\leq$295 Ma) either represents a new magmatic pulse or fluid invasion (M_3).
- M_2 metamorphism and extensional D_2 deformation were not related with the collisional evolution of the crust, but are probably associated with a crustal-scale,

dextral shear zone, which admitted the advection of heat by hot, low-viscosity solids and/or by melts.

- A negative gravity anomaly centered around the Zone Axiale suggests that the bulk of these melts were granitic, although mafic intrusions into the lower crust are required as the ultimate heat source.
- Similar "hot" core complexes with the same age clusters occur both in northern parts of the Massif Central and in the Pyrenees, irrespective of their different positions in the orogen. Coeval magmatic pulses are also known from the Massif de Maures and SW Germany. These large-scale relationships support the idea that extension and advection of heat from the mantle are not directly related to the Variscan collision, but to a system of dextral strike slip faults along which Gondwana moved westwards with respect to Laurussia, thus opening the Palaeotethys ocean.

Acknowledgments We acknowledge funding by Deutsche Forschungsgemeinschaft (Fr 668/24). We are also indebted to helpful discussions with H. Echtler (Potsdam), P. Matte (Montpellier) and E. Stein (Darmstadt). Comments of an anonymous reviewer, by Michel Faure and Claudio Rosenberg have done much to improve the manuscript. We would also like to thank W. Dörr and J. Schastok for their help with isotopic dating. B. Rotthaus collected the geochronolgy samples coded "BR" and separated the micas.

References

Ábalos B, Carreraas J, Druguet E, Escuder Viruete J, Gómez Pugnaire MT, Alvarez SL, Quesada C, Rodríguez Fernández LR, Gil-Ibarguchi JI (2002) Variscan and pre-Variscan tectonics. In: Gibbons W, Moreno T (eds) The geology of Spain. The Geological Society, London, pp 155–183

Aerden DGAM (1998) Tectonic evolution of the Montagne Noire and a possible orogenic model for for syn-collisional exhumation of deep rocks, Hercynian belt, France. Tectonics 17:62–79

Aerden DGAM, Malavieille J (1999) Origin of a large-scale fold nappe in the Montagne Noire, Variscan Belt, France. J Struct Geol 21:1321–1333

Alabouvette B, Arthaud F, Bambier A, Freytet P, Paloc H (1981) Carte Géologique de la France No. 1014, St. Chinian, 1:50,000 et notice explicative. Bureau de Recherches Géologiques et Minières. Notice explicative, pp 1–44

Alabouvette B, Demange M, Sauvel C, Vautrelle C (1982) Carte Géologique de la France No. 1013, St. Pons, 1:50,000 et notice explicative. Bureau de Recherches Géologiques et Minières. Notice explicative, pp 1–123

Alabouvette B, Demange M, Guérangé-Lozes J, Ambert P (2003) Carte Géologique de la France No. 38, Montpellier, 1:250000 et notice explicative. Bureau de Recherches Géologiques et Minières. Notice explicative, pp 1–164

Aretz M (2002) Habitatanalyse und Riffbildungspotential kolonialer rugoser Korallen im Unterkarbon (Mississippium) von Westeuropa. Kölner Forum für Geologie und Paläontologie 10:1–155

Arthaud F (1969) Un example de relation entre l'étirement dans B dans la dispersion des linéations et la courbure des axes des plis (versant Sud de la Montagne Noire). Revue de Géographique Physique et de Géologie Dynamique 11:523–532

Arthaud F (1970) Etude tectonique et microtectonique comparée de deux domaines Hercyniens: Les nappes de la Montagne Noire (France) et l'Anticlinorium de l'Iglesiente (Sardaigne). Publications USTELA, Série Géologie Structurale 1:1–175

Arthaud F, Matte P (1975) Late-Paleozoic strike-slip faulting in southern Europe and northern Africa: result of a right lateral shear zone between the Appalachians and the Urals. Geol Soc Am Bull 88:1305–1320

Babeyko YA, Sobolev SV, Trumbull RB, Oncken O, Lavier LL (2002) Numerical models of crustal scale convection and partial melting beneath the Altiplano-Puna plateau. Earth Planet Sci Lett 199:373–388

Bard JP, Rambeloson R (1973) Métamorphisme plurifacial et sens de variation du degré géothermique durant la tectogenèse polyphasée hercynienne dans la partie orientale de la Zone Axiale de la Montagne Noire (Massif du Caroux, Sud du Massif Central Français). Bulletin de la Société géologique de France 7:579–586

Be Mezeme E (2005) Contribution de la géochronologique U–Th–Pb sur Monazite à la compréhension de la fusion crustale de la chaîne Varisque Française et implication géodynamique. Unpublished PhD thesis, Orléans, pp 1–277

Be Mezeme E, Faure M, Chen Y, Cocherie A, Talbot J-Y (2007) Structural, AMS and geochronological study of a laccolith emplaced during Late Variscan orogenic extension: the Rocles pluton (SE French Massif Central). Int J Earth Sci 96:215–228

Béaud F (1985) Etude structurale de la zone axiale orientale de la Monagne Noire (Sud de Massif Central Français). Détermination des mécanismes de déformation, relation avec les nappes du versant sud. Thèse Université des Sciences et Techniques du Languedoc, pp 1–190

Blatt AKH, Dörr W, Stein E (2005) Neoproterozoic basement in the metasedimentary envelope of the Zone Axiale of the Montagne Noire (S-France). Poster, Annual Meeting of Geologische Vereinigung, Erlangen 2005

Bogdanoff S, Donnot M, Ellenberger F (1984) Carte Géologique de la France No. 988, Bédarieux, 1:50,000 et notice explicative. Bureau de Recherches Géologiques et Minières. Notice explicative, pp 1–106

Bouchot V, Milési JP, Lescuyer JL, Ledru P (1997) Les minéralisations aurifères de la France dans leur cadre géologique autour de 300 Ma. Chron Rech Min 528:13–62

Brichau S, Respaut J-P, Monié P (2008) New age constraints on empacement of the Cévenol granitoids, South French Massif Central. Int J Earth Sci (Geologische Rundschau) 97:725–738

Bruguier O, Becq-Giraudon JF, Champenois M, Deloule E, Ludden J, Mangin D (2003) Application of in situ zircon geochronology and accessory phase chemistry to constraining basin development during post-collisional extension: a case study from the French Massif Central. Chem Geol 201:319–336

Burg JP, Gerya TV (2005) The role of viscous heating in Barrovian metamorphism of collisional orogens: thermomechanical models and application to the Lepontine Dome in the Central Alps. J Met Geol 23:75–95

Cassard D, Feybesse J-L, Jean-Luc L (1993) Variscan crustal thickening, extension and late overstacking during the Namurian-Westphalian in the western Montagne Noire (France). Tectonophysics 222:33–53

Castro A, Corretgé G, de la Rosa J, Enrique P, Martínez FJ, Pascual E, Lago M, Arranz E, Galé C, Fernández C, Donaire T, López S (2002) Palaeozoic magmatism. In: Gibbons W, Moreno T (eds) The geology of Spain. The Geological Society, London, pp 117–153

Charles N, Faure M, Chen Y (2009) The Montagne Noire migmatitic dome emplacement (French Massif Central): new insights from

petrofabric and AMS studies. J Struct Geol 31:1423–1440. doi: 10.1016/j.jsg.2009.08.007

Cocherie A, Baudin T, Autran A, Guerrot C, Fanning CM, Laumonier B (2005) U–Pb zircon (ID-TIMS and SHRIMP) evidence for the early ordovician intrusion of metagranites in the laste Proterozoic Canaveilles Group of the Pyrenees and the Montagne Noire (France). Bull Soc Géol France 176:269–282

Cogné J (1990) The Cadomian Orogeny and its influence on the Variscan evolution of western Europe. In: D′Lemos RS, Strachan RA, Topley CG (eds) The Cadomian Orogeny. Geological Society Special Publications, vol 51, pp 305–311

Colmenero JR, Fernández LP, Moreno C, Bahamonde JR, Barba P, Heredia N, González F (2002) Carboniferous. In: Gibbons W, Moreno T (eds) The geology of Spain. The Geological Society, London, pp 93–116

Corpel J, Debeglia N, Guérangé-Lozes (1987) Apport de la gravimétrie à la cartographie géologique et structurale de l'Albigeois: Rapport de Bureau de Recherches Géologique et Minière, vol 87, DT 015 GPH

Corsini M, Bosse V, Demoux A, Billo S, Féraud G, Lardeaux JM, Rolland Y, Schärer U (2004) Late orogenic HT-metamorphism and exhumation during ongoing convergence in the Hercynian Tanneron Massif, France. RST, GV Conference Abstract

Costa S (1990) De la collision continentale à l'extension tardi-orogénique: 100 millions d'années d'histoire varisque dans le Massif Central français. Une étude chronologique par la méthode 40Ar-39Ar. Thesis, University of Languedoc, Montpellier, pp 1–391

Costa S, Rey P (1995) Lower crustal rejuvenation and growth during post thickening collapse: insigths from a crustal cross section through a Variscan metamorphic core complex. Geology 23:905–908

Demange M (1985) The eclogite-facies rocks of the Montagne Noire, France. Chem Geol 50:173–188

Demange M (1998) Contribution au problème de la formation des dômes de la zone axiale de la Montagne noire: analyse géométrique des plissements superposés dans les séries métasédimentaires de l'enveloppe. Implications pour tout modèle géodynamique. Géologie de la France 4:3–56

Demange M (1999) Évolution tectonique de la Montagne noire: un modèle en transpression. Comptes Rendus de l′Académie des sciences. Paris Série, IIa 329:329–823

Demange M, Guérangé-Lozes J, Guérangé B (1995) Carte Géologique de la France No. 987, Lacaune, 1:50,000 et notice explicative. Bureau de Recherches Géologiques et Minières. Notice explicative, pp 1–153

Demoux A, Schärer U, Corsini M (2008) Variscan evolution of the Tanneron massif, SE France, examined through U–Pb monazite ages. J Geol Soc Lond 165:467–478

Dörr W, Fiala J, Vejnar Z, Zulauf G (1998) U–Pb zircon ages and structural development of metagranitoids of the Teplá Crystalline Complex: evidence for pervasive Cambrian plutonism within the Bohemian Massif (Czech Republic). Geol Rundschau 87:135–149

Dörr W, Zulauf G, Fiala J, Franke W, Vejnar Z (2002) Neoproterozoic to Early Cambrian history of an active plate margin in the Teplá Barrandian unit—a correlation of U–Pb Isotopic-Dilution-TIMS ages (Bohemia, Czech Republic). Tectonophysics 352:65–85

Doublier MP (2000) Diplomkartierung im Bereich des Südflügels der Montagne Noire nördlich von Le Lau (Montagne Noire). Inst. für Geowissenschaften der Justus Liebig-Universität Gießen, pp 1–56

Doublier MP (2007) Die tektono-metamorphe Entwicklung der sehr niedergradigen paläozoischen Sedimente der Montagne Noire (Südfrankreich). Dissertation, Goethe University Frankfurt a. Main, pp 1–373, http://deposit.ddb.de/cgi-bin/dokserv?idn=984987614

Doublier MP, Potel S, Wemmer K (2006) Age and grade of metamorphism in the eastern Monts de Lacaune–implications for the collisional accretion in Variscan externides (French Massif Central). Geodinamica Acta 19:391–407

Duthou J-L, Cantagrel JM, Didier J, Vialette Y (1984) Palaeozoic granitoids from the French Massif Central: age and origin studied by 87Rb/87Sr system. Phys Earth Planet Interiors 35:131–144

Echtler H (1990) Geometry and kinematics of recumbent folding and low-angle detachment in the Pardailhan nappe (Montagne Noire, Southern French Massif Central). Tectonophysics 177:109–123

Echtler H, Malavieille J (1990) Extensional tectonics, basement uplift and Stephano-Permian collapse basin in a Late Variscan metamorphic core complex (Montagne Noire, Southern Massif Central). Tectonophysics 177:125–138

Engel W (1984) Migration of folding and flysch sedimentation on the southern flank of the Variscan belt (Montagne Noire, Mouthoumet Massif, Pyrenees). Zeitschrift der Deutschen Geologischen Gesellschaft 135:279–292

Engel W, Feist R, Franke W (1978) Synorogenic gravitational transport in the Montagne Noire (S-France). Zeitschrift der Deutschen Geologischen Gesellschaft 129:461–472

Engel W, Feist R, Franke W (1981) Le Carbonifère anté-Stéphanien de la Montagne Noire: rapport entre mise en place des nappes et sédimentation. Bulletin du Bureau des Recherches Géologiques et Minières 1(4):341–389

Faure M (1995) Late orogenic Carboniferous extension in the Variscan French Massif Central. Tectonics 14:132–153

Faure M, Cottereau N (1988) Données cinématiques sur la mise en place du dôme migmatitique carbonifère moyen de la zone axiale de la Montagne Noire (Massif Central, France). Comptes Rendus de l′Académie des sciences, Paris, Série IIa 307:1787–1794

Faure M, Pons J (1991) Crustal thinning recorded by the shape of the Namurian-Westphalian leucogranite in the Variscan belt of the northwest Massif Central, France. Geology 19:730–733

Faure M, Monié P, Pin C, Maluski H, Leloix C (2002) Late Viséan thermal event in the northern part of the French Massif Central: new 40Ar/39Ar and Rb-Sr isotopic constraints on the Hercynian syn-orogenic extension. Int J Earth Sci (Geologische Rundschau) 91(1):53–75

Faure M, Lardeaux J-M, Ledru P (2009) A review of the pre-Permian geology of the Variscan French Massif Central. Comptes Rendus Geosci 341:202–213

Feist R (1985) Devonian Stratigraphy of the Southeastern Montagne Noire. Courier Forschungsinstitut Senckenberg 75:331–352

Feist R, Galtier J (1985) Découverte de flores d'âge namurien probable dans le flysch à olistolites de Cabrières (Hérault). Implication sur la durée de la sédimentation synorogénique dans la Montagne Noire. Comptes Rendus de l′Académie des sciences, Paris, Série IIa 300:207–212

Feist R, Schönlaub HP (1974) Zur Silur/Devon-Grenze in der östlichen Montagne Noire Süd-Frankreichs. N J Geol Paläont Mh 4:200–219

Feist R, Echtler H, Galtier J, Mouthier B (1994) Biostratigraphy and Dynamics of the Nonmetamorphic Sedimentary Record. In: Keppie (Ed): Pre-Mesozoic Geology in France and related areas. Springer, Berlin, pp 289–304

Franke W (2001) Exhumation of LP gneisses in the Montagne Noire (S-France): The collapse has collapsed. J Conf Abst 61(EUG XI):235

Franke, W (2009) Orogen meets Rift: Causes of Late Variscan HT Processes. Abstracts GV Annual Meeting 2009, Göttingen, p 35

Franke W, Doublier MP, Königshof P, Wiederer U (2000) Exhumation of an anatectic gneiss dome: news from the Montagne Noire (S-France). Abstracts Basement Tectonics 15 (Galicia 2000)

Gardien V, Lardeaux JM, Ledru P, Allemand P, Guillot S (1997) Metamorphism during late orogenic extension: insights from the French Variscan belt. Bulletin de la Société géologique de France 168:271–286

Gebauer D, Grünenfelder M (1976) U–Pb zircon and Rb–Sr whole-rock dating of low-grade metasediments, example: Montagne Noire (Southern France). Contrib Mineral Petrol 59:13–32

Gebauer D, Compston W, Williams IS, Grünenfelder M (1988) U–Pb zircon ion-probe dating of augengneisses of the Montagne Noire and the significance of the Caledonian subcycle in the French massif central. In: Terranes in the Variscan belt of France and western Europe, Abstract Volume

Gèze B (1949) Étude géologique de la Montagne Noire et des Cévennes méridionales. Mémoires de la Société géologique de France 62:1–215

Gèze B, de Sitter LU, Trümpy R (1952) Sur le sens de déversement des nappes de la Montagne Noire. Bulletin de la Société géologique de France 7:491–535

Gleizes G, Crevon G, Asrat A, Barbey P (2006) Structure, age and mode of emplacement of the Hercynian Bordères-Louron pluton (Central Pyrenees, France). Int J Earth Sci 95:1039–1052

Gonord H, Ragot JP, Saugy L (1964) Observations lithostratigraphiques nouvelles sur la série de base (Ordovicien inférieur) des nappes de Cabrières, région de Gabian-Glauzy (Montagne Noire, Hérault). Bulletin de la Société géologique de France 6:419–427

Gradstein FM, Ogg JG, Smith AG (2004) A geologic time scale 2004, vol XIX. Cambridge University Press, Cambridge, pp 1–589

Grow JA, Bowin C (1975) Evidence for high-density crust and mantle beneath the Chile Trench due to the descending lithosphere. J Geophys R 80:1449–1458

Guérangé-Lozes J, Burg JP (1990) Les nappes varisques du sud-ouest du Massif central (cartes géologiques et structurales à 1/250,000 Montpellier et Aurillac). Géologie de la France 3–4:71–106

Hamet J, Allègre CJ (1976) Hercynian orogeny in the Montagne Noire (France): application of Rb/Sr systematics. Bull Geol Soc Am 87:1429–1442

Henk A, von Blanckenburg F, Finger F, Schaltegger U, Zulauf G (2000) Syn-convergent high-temperature metamorphism and magmatism in the Variscides: a discussion of potential heat sources. In: Franke W, Haak V, Oncken O, Tanner D (eds) Orogenic processes: quantification and modelling in the Variscan Belt. Geol Soc Spec Publ 179:387–400

Holland TJB, Powell R (1998) An internally-consistent thermodynamic dataset for phases of petrological interest. J Metamorph Geol 16:309–344 internet update: 2001

Hollinger P, Cuney M, Friedrich M, Turpin L (1986) Age carbonifère de l′unité de Brame du complexe granitique peralumineux de Saint-Sylvestre (NO du Massif Central) défini par les données isotopiques U–Pb sur zircon et monazite. Comptes Rendus Acadademie des Sciences, Paris, II 303:1309–1314

Keller L, Fügenschuh B, Hess B, Schneider B, Schmid SM (2006) Simplon fault zone in the western and central Alps: mechanism of Neogene faulting and folding revisited. Geology 34:317–320

Klama K (2001) U–Pb-Datierungen von Einzelzirkonen und -Monaziten aus syn- und posttektonischen Granitoiden im Caroux-Massiv der Axialzone (Montagne Noire, Südfrankreich): Unpubl. Diploma Thesis, Justus Liebig-Universität Giessen, pp 1–76

Klama K, Dörr W, Franke W (2001) Exhumation of LP gneisses in the Montagne Noire (S-France): isotopic constraints. J Conf Abst 61(EUG XI):235

Krause J, Dörr W, Stein E (2004) Wenn man es zu genau wissen will. Oder: Wenn die Intrusion nicht zur Kontaktmetamorphose passt—ein Beispiel aus der Montagne Noire. Terra Nostra 2004/1, p 48

Ledru P, Courrioux G, Lardeaux JM, Montel JM, Vanderhaeghe O, Vitel G (2001) The Velay dome (French Massif Central): melt generation and granite emplacement during orogenic evolution. Tectonophysics 342:207–237

Lee B-J, Faure M, Cluzel D, Cadet J-P (1988) Mise en évidence d'un cisaillement ductile d'ouest en est dans les nappes du versant sud de la Montagne Noire (sud du Massif Central). Comptes Rendus de l′Académie des sciences, Paris, Série IIa, vol 306, pp 455–462

Lescuyer L, Cocherie A (1992) Datation sur monozircons des métadacites de Sériès: arguments pour un âge protérozoïque terminal des "schistes X" de la Montagne Noire (Massif central français). Comptes Rendus de l′Académie des sciences, Paris. Série IIa 314(2):1071–1077

Lévêque J (1986) Caractérisation isotopique de processus hydrothermaux au niveaux d'un apex granitique: le Folat (NE de la Montagne Noire). Conférence Abstract, 11ème Réunion Annuelle des Sciences de la Terre, p 112

Lister GS, Baldwin SL (1993) Plutonism and the origin of metamorphic core complexes. Geology 21:607–610

Maluski H, Costa S, Echtler H (1991) Late Variscan tectonic evolution by thinning of earlier thickened crust. An ^{40}Ar-^{39}Ar study of the Montagne Noire, southern Massif Central, France. Lithos 26:287–304

Mancktelow NS, Pavlis TL (1994) Fold-fault relationships in low-angle detachment systems. Tectonics 13(2):668–685

Mattauer M (2004) Orthogneisses in the deepest levels of the Variscan belt are not a Precambrian basement but Ordovician granites: tectonic consequences. Comptes Rendus Geosci 336:487–489

Mattauer M, Laurent Ph, Matte Ph (1996) Plissement hercynien synschisteux post-nappe et étirement subhorizontal dans le versant sud de la Montagne Noire (Sud du Massif Central, France). Comptes Rendus de l′Académie des sciences, Paris, Série IIa 322:309–315

Matte P (1991) Accretionary history and crustal evolution of the Variscan belt in Western Europe. Tectonophysics 196:309–337

Matte P, Lancelot J, Mattauer M (1998) La zone axiale hercynienne de la Montagne Noire n'est pas un "metamorphic core complex" extensif mais un anticlinal post-nappe à cœur anatectique. Geodinamica Acta 11(1):13–22

Maurel O, Respaut J-P, Monié P, Arnaud N, Brunel M (2004) U–Pb emplacement and 40Ar/39Ar cooling ages of the eastern Mont-Louis granite massif (Eastern Pyrenees, France). Comptes Rendus Geosci 336:1091–1098

Mezger JE, Passchier CW (2003) Polymetamorphism and ductile deformation of staurolite-cordierite schist of the Bossòst dome: indication for Variscan extension in the Axial Zone of the central Pyrenees. Geol Mag 150:595–612

Mialhe J (1980) Le masif granitique de la Borne (Cévennes). Étude petrographique, géochimique, géochronologique et structurale. PhD thesis, Université de Clermont-Ferrand, pp 1–171

Miyazaki K (2004) Low-P–high-T metamorphism and the role of heat transport by melt migration in the Higo Metamorphic Complex, Kyushu, Japan. J Metamorph Geol 22:793–809

Monié P, Respaut J P, Brichaud S, Bouchot V, Faure M, Roig J Y (2000) 40Ar/39Ar and U–Pb geochronology applied to Au-W-Sb metallogenesis in the Cévennes and Châtaigneraie districts (Southern Masif Central, France). In: Orogenic Gold deposits in Europe, Document BRGM 297. Bureau de Recherches Géologiques et Minières, Orléans, France, pp 77–79

Montel JM, Bouloton J, Veschambre M, Pellier C, Ceret K (2002) Âges stéphaniens des microgranites du Velay (Massif central francais). Géologie de la France 1:15–20

Mougeot R, Respaut J-P, Ledru P, Marignac C (1997) U–Pb chronology on accessory minerals of the Velay anatectic dome (French Massif Central). Eur J Mineral 9:141–156

Nicholas A, Bouchez JL, Blaise J, Poirier JP (1977) Geological aspects of deformation in continental shear zones. Tectonophysics 42:55–73

Olivier Ph, Gleizes G, Paquette JL (2004) Gneiss domes and granite emplacement in oblique convergence regime. New interpretation of the Variscan Agly massif (Eastern Pyrenees, France). In: Whitney DL, Teyssier C, Siddoway CS (eds) Gneiss Domes and Orogeny. Geol. Soc. America Spec. Paper, vol 380, pp 229–242

Olivier Ph, Gleizes G, Paquette J-L, Muñoz Sáez C (2008) Structure and U–Pb dating of the Saint-Arnac pluton and the Ansignan charnockite (Agly Massif): a cross-section from the upper to the middle crust of the Variscan Eastern Pyrenees. J Geol Soc Lond 165:141–152

Ourzik A, Debat P, Mercher A (1991) Évolution métamorphique de la partie N et NE de la zone axiale de la Montagne Noire (Sud du Massif Central, France). Comptes Rendus de l′Académie des sciences, Paris, Série IIa 313:1547–1553

Paquette JL, Gleizes G, Leblanc D, Bouchez JL (1997) Le granite de Bassiès (Pyrenées): un pluton syntectonique d′âge westphalien. Géochronologie U–Pb sur zircons. Comptes Rendus de l′Académie des sciences. Paris 324:387–392

Paris F, Le Pochat G (1994) The Aquitaine basin. In: Keppie JD (ed) Pre-Mesozoic geology in France and related areas. Springer, Berlin, pp 405–415

Petford N, Cruden AR, Mc Caffrey KJW, Vigneresse J-L (2000) Granite magma formation, transport and emplacement in the earth's crust. Nature 408:669–673

Pin C (1989) Essai sur la chronologie et l′évolution géodynamique de la chaîne hercynienne d′Europe. PhD thesis, Blaise Pascal University, Clermont-Ferrand

Pin C, Vielzeuf D (1983) Granulites and related rocks in Variscan median Europe: a dualistic interpretation. Tectonophysics 93:47–74

Piqué A, Bogdanoff S, Quénardel J-M, Rolet J, Santallier D (1994) The French Paleozoic terranes. In: Keppie JD (ed) Pre-Mesozoic Geology in France and related areas. New York, Springer, pp 483–500

Postaire B (1982) Systématique Pb commun et U–Pb sur zircons. PhD thesis, University of Rennes

Respaut JP, Lancelot JR (1983) U–Pb dating on zircons and monazites of the synmetamorphic emplacement of the Ansignan charnockite (Agly Massif, France). Neues Jahrbuch für Mineralogie, Abhandlungen 147:21–34

Rey PF, Teyssier C, Whitney DL (2009) The role of partial melting and extensional strain rates in the development of metamorphic core complexes. Tectonophysics 477:135–144

Ring U, Gessner K, Brichau S, Glodny J (2004) Some like it hot! Core complex formation on Naxos and Ios islands, Aegean Sea, Greece. RST-GV Conference Abstract

Roberts MP, Pin C, Clemens JD, Paquette JL (2000) Petrogenesis of mafic to felsic plutonic rock associations: the calc-alkaline Quérigut complex, French Pyrenees. J Petrol 41:809–844

Roger F, Respaut J-P, Brunel M, Ph Matte, Paquette J-L (2004) Première datation U–Pb des orthogneiss oeillés de la zone axiale de la Montagne Noire (Sud du Massif Central): nouveaux témoins du magmatisme ordovicien dans la chaîne Varisque. Comptes Rendus Geosci 336:19–28

Romer RL, Soler A (1995) U–Pb age and and lead isotopic characterization of Au-bearing skarn related to the Andorra granite (Pyrenees, Spain). Mineralium Deposita 30:374–383

Roques M (1941) Les schistes cristallins de la partie sud-ouest du Massif Central français. Mémoires d′Explication de la Carte géologique de France, pp 1–527

Rosenberg CL, Brun JP, Gapais D (2004) Indentation model of the Eastern Alps and the origin of the Tauern Window. Geology 32:997–1000

Schaltegger U (1997) Magma pulses in the Central Variscan Belt: episodic melt generation and emplacement during lithospheric thinning. Terra Nova 9:242–245

Schaltegger U, Brack P (2007) Crustal-scale magmatic systems during intracontinental strike-slip tectonics: U, Pb and Hf isotopic constraints from Permian magmatic rocks of the Southern Alps. Int J Earth Sci (Geologische Rundschau) 96:1131–1151

Schranzhofer C (1999) La zone de cisaillement polyphasee du versant sud de la zone axiale de la Montagne Noire (Massif Central, France): Un "vecteur" pour l'exhumation des domes migmatitiques. Thesis, Institut Geologique Albert de Lapparent, Universite Paris VI—Pierre et Marie Curie, pp 1–203

Schuiling RD, de Widt MJ (1962) Sur la genèse du dôme gneissique de l'Agout (Dépts. Tarn et Hérault). Geologie en Mijnbouw 41:321–326

Soula J-C, Debat P, Brusset S, Bessière G, Christophoul F, Déramond J (2001) Thrust-related, diapiric, and extensional doming in a frontal orogenic wedge: example of the Montagne Noire, Southern French Hercynian Belt. J Struct Geol 23:1677–1699

Talbot J-Y, Guillaume M, Courrioux G, Chen Y, Faure M (2004) Emplacement in an extensional setting of the Mont Lozère granitic complex (SE France) inferred from comprehensiv AMS, structural and gravity studies. J Struct Geol 26:11–28

Teyssier C, Whitney DL (2002) Gneiss domes and orogeny. Geology 30:1139–1142

Thompson PH, Bard J-P (1983) Isograds and mineral assemblages in the eastern axial zone, Montagne Noire (France): implications for the temperature gradients and P-T history. Can J Earth Sci 19:129–143

Van Den Driessche J, Brun JP (1989) Un modèle cinématique de l′extension Paléozoique supérieur dans le Sud du Massif Central. Comptes Rendus de l′Académie des sciences, Paris, Série IIa 309:1607–1613

Van Den Driessche J, Brun JP (1992) Tectonic evolution of the Montagne Noire (French Massif Central): a model of extensional gneiss dome. Geodinamica Acta 5:85–99

Van Hinsberg VJ, Zinngrebe E, De Wijs H, Vriend SP (2007) Thermo-chronology of the Barlet metamorphic basement unit: evidence for a Stephanian thermal event linked to Sb mineralizations in the Haut Allier, France. J Geol Soc Lond 164(2): 393–404

Vanderhaege O, Burg JP, Teyssier C (1999). Exhumation of migmatites in two collapsed orogens: Canadian Cordillera and Frech Variscides. In: Ring U, Brandon MT, Lister GS, Willet SD (eds) Exhumation processes: normal faulting, ductile flow and erosion. Geological Society Special Publication, vol 154, pp 181–204

Vilà M, Pin C, Liesa M, Enrique P (2007) LP-HT metamorphism in a late orogenic transpressional setting, Albera Massif, NE Iberia: implications for the geodynamic evolution of the Variscan Pyrenees. J Metamorph Geol 25(3):321–348

Villa IM (1998) Isotopic closure. Terra Nova 10:42–47

Vitrac-Michard A, Allègre CJ (1975) A study of the formation and history of a piece of continental crust by the ^{87}Rb-^{87}Sr method: the case of the French Oriental Pyrenees. Contrib Mineral Petrol 50:257–285

Von Blanckenburg F, Villa IM, Baur H, Morteani G, Steiger RH (1989) Time calibration of a PT-path from the Western Tauern Window, Eastern Alps: the problem of closure temperatures. Contrib Mineral Petrol 101:1–11

Wemmer K (1991) K–Ar Altersdatierungsmöglichkeiten für retrograde Deformationsprozesse im spröden und duktilen Bereich–Beispiele aus der KTB-Vorbohrung (Oberpfalz) und dem Bereich der Insubrischen Linie (N-Italien). Göttinger Arbeiten für Geologie und Paläontologie 51:1–61

Weyer D, Menning M (2006) Geologische Zeitskala, stratigraphische Nomenklatur und Magnetostratigraphie. In: Deutsche Stratigraphische Kommission (Herausgabe, Koordination und Redaktion: Amler MRW, Stoppel D für die Subkommission Karbon): Stratigraphie von Deutschland VI—Unterkarbon (Mississippium). Schriftenreihe der deutschen Gesellschaft für Geowissenschaften 41:27–50

Wickham SM, Oxburgh ER (1985) Continental rifts as a setting for regional metamorphism. Nature 318:330–333

Wiederer U, Königshof P, Feist R, Franke W, Doublier MP (2002) Low-grade metamorphism in the Montagne Noire (S-France): Conodont Alteration Index (CAI) in Palaeozoic carbonates and implications for the exhumation of a hot metamorphic core complex. Schweiz Mineral Petrogr Mitt 82:393–407

Willigers BJA, Krogstad EJ, Wijbrans JR (2001) Comparison of thermochronometers in a slowly cooled granulite terrain: Nagsugtoqidian Orogen, West Greenland. J Petrol 42/9:1729–1749